การสังเคราะห์อนุภาคซิลิการะดับนาโนเมตรที่กราฟต์ด้วยโคบาลามินสำหรับเซลล์มะเร็งเป้าหมาย

นางสาวณัฏฐนิฎา เทพพันธ์กุลงาม

วิทยานิพนธ์นี้เป็นส่วนหนึ่งของการศึกษาตามหลักสูตรปริญญาวิทยาศาสตรมหาบัณฑิต
สาขาวิชาเคมี ภาควิชาเคมี
คณะวิทยาศาสตร์ จุฬาลงกรณ์มหาวิทยาลัย
ปีการศึกษา 2558

SYNTHESIS OF COBALAMIN-GRAFTED SILICA NANOPARTICLES FOR TARGETING CANCER CELLS

Miss Nattanida Thepphankulngarm

A Thesis Submitted in Partial Fulfillment of the Requirements
for the Degree of Master of Science Program in Chemistry
Department of Chemistry
Faculty of Science
Chulalongkorn University
Academic Year 2015

Thesis Title	SYNTHESIS OF COBALAMIN-GRAFTED SILICA NANOPARTICLES FOR TARGETING CANCER CELLS
By	Miss Nattanida Thepphankulngarm
Field of Study	Chemistry
Thesis Advisor	Professor Thawatchai Tuntulani, Ph.D.
Thesis Co-Advisor	Pannee Leeladee, Ph.D.

Accepted by the Faculty of Science, Chulalongkorn University in Partial Fulfillment of the Requirements for the Master's Degree

.....Dean of the Faculty of Science
(Associate Professor Polkit Sangvanich, Ph.D.)

THESIS COMMITTEE

.....Chairman
(Associate Professor Vudhichai Parasuk, Ph.D.)

.....Thesis Advisor
(Professor Thawatchai Tuntulani, Ph.D.)

.....Thesis Co-Advisor
(Pannee Leeladee, Ph.D.)

.....Examiner
(Numpon Insin, Ph.D.)

.....Examiner
(Nawaporn Vinayavekhin, Ph.D.)

.....External Examiner
(Chaweewan Sapcharoenkun, Ph.D.)

ณัฏฐนิฎา เทพพันธ์กุลงาม : การสังเคราะห์อนุภาคซิลิการะดับนาโนเมตรที่กราฟต์ด้วยโคบาลามินสำหรับเซลล์มะเร็งเป้าหมาย (SYNTHESIS OF COBALAMIN-GRAFTED SILICA NANOPARTICLES FOR TARGETING CANCER CELLS) อ.ที่ปรึกษาวิทยานิพนธ์หลัก: ศ. ดร.ธวัชชัย ตันฑุลานิ, อ.ที่ปรึกษาวิทยานิพนธ์ร่วม: ดร.พรรณี ลีลาดี, 79 หน้า.

การบำบัดอย่างจำเพาะเจาะจงได้รับการพัฒนามาอย่างต่อเนื่องเพื่อที่จะช่วยลดผลข้างเคียงจากยารักษามะเร็ง โดยการนำส่งยาเข้าสู่เฉพาะเซลล์มะเร็งเท่านั้น ในงานวิจัยนี้ผู้วิจัยสามารถสังเคราะห์ระบบนำส่งยาชนิดใหม่เพื่อให้มีความจำเพาะต่อเซลล์มะเร็งได้สำเร็จ ระบบนี้ประกอบด้วยอนุภาคซิลิกาที่ใช้เป็นวัสดุในการบรรจุและขนส่งยา ซิสพลาติน (CDDP) ที่ใช้เป็นยารักษามะเร็ง และโคบาลามิน (Cbl) ที่ใช้เป็นโมเลกุลเป้าหมายในการนำระบบยาไปสู่เซลล์มะเร็ง ในขั้นตอนแรกได้สังเคราะห์อนุภาคซิลิกา (PSNs, 1) ด้วยวิธีโซล-เจล แต่พบว่าเมื่อวิเคราะห์ด้วยเทคนิค ICP-AES อนุภาค (1) สามารถบรรจุซิสพลาตินได้เพียง 7% เท่านั้น จึงได้ดัดแปรพื้นผิวของอนุภาคซิลิกาให้เป็นหมู่คาร์บอกซิล ซึ่งอนุภาคชนิดนี้ (PSNsCOOH, 2) สามารถบรรจุซิสพลาตินได้มากถึง 59% จากนั้นจึงนำโมเลกุลเป้าหมาย Cbl-CDDP มากราฟต์บนอนุภาค CDDP@PSNsCOOH (3) ได้เป็น CDDP@CblPSNsCOOH (4) สามารถพิสูจน์เอกลักษณ์ของอนุภาคดังกล่าวด้วยเทคนิคการเลี้ยวเบนรังสีเอ็กซ์ (XRD) อินฟราเรดสเปกโทรสโกปี (IR) ยูวี-วิสิเบิลสเปกโทรสโกปี (UV-vis) กล้องจุลทรรศน์อิเล็กตรอนแบบส่องกราด (SEM) และ นาโนไซส์เซอร์ (nanosizer) จากผลการทดลองพบว่า อนุภาค (4) มีลักษณะเป็นทรงกลมและกระจายตัวอย่างสม่ำเสมอ มีขนาดเส้นผ่านศูนย์กลางเฉลี่ยเท่ากับ 316 นาโนเมตร เพื่อจำลองปฏิกิริยารีดักชั่นในเซลล์มะเร็ง การศึกษาการปลดปล่อยยาที่ pH 5.5 พบว่าการรีดิวซ์อนุภาค (4) ด้วย $NaBH_4$ ให้ผลิตภัณฑ์เป็น $[Co^{2+}(Cbl)]$ ช่วยเหนี่ยวนำให้เกิดการปลดปล่อยยาได้ดียิ่งขึ้น การทดลองนี้ชี้ให้เห็นว่านอกจากโมเลกุล Cbl จะสามารถทำหน้าที่เป็นโมเลกุลเป้าหมายเพื่อเพิ่มความจำเพาะเจาะจงต่อเซลล์มะเร็งได้แล้ว ยังสามารถช่วยป้องกันการปลดปล่อยยาออกจากอนุภาคก่อนถึงเซลล์เป้าหมายได้อีกด้วย

ภาควิชา เคมี	ลายมือชื่อนิสิต .....
สาขาวิชา เคมี	ลายมือชื่อ อ.ที่ปรึกษาหลัก .....
ปีการศึกษา 2558	ลายมือชื่อ อ.ที่ปรึกษาร่วม .....

5671953723 : MAJOR CHEMISTRY

KEYWORDS: TARGETED DRUG DELIVERY SYSTEM / CYANOCOBALAMIN / SILICA NANOPARTICLES / CISPLATIN

NATTANIDA THEPPHANKULNGARM: SYNTHESIS OF COBALAMIN-GRAFTED SILICA NANOPARTICLES FOR TARGETING CANCER CELLS. ADVISOR: PROF. THAWATCHAI TUNTULANI, Ph.D., CO-ADVISOR: PANNEE LEELADEE, Ph.D., 79 pp.

Targeted therapy has been developed to reduce side effects of anticancer agents by specific localization of the drug to target only the cancer cells. In this thesis, a novel drug delivery system for targeting cancer cells was successfully synthesized. The system consisted of porous silica nanoparticle as the drug vehicle, cisplatin (CDDP) as the drug model, and cobalamin (Cbl) as the targeting molecule for cancer cells. Porous silica nanoparticle (PSNs, 1) were firstly prepared by sol-gel method, but the drug-loading capacity was only 7% as determined by ICP-AES. Thus, surface modification of PSNs with pendent carboxyl groups was carried out to obtain carboxyl-porous silica nanoparticles (PSNsCOOH, 2), of which the drug-loading capacity notably increased up to 59%. Then, the targeting molecule, $[Cbl\text{-}CDDP]^{+}$ was grafted on CDDP@PSNsCOOH (3), resulting in CDDP@CblPSNsCOOH (4). The obtained particles were characterized by various techniques including XRD, IR, UV-vis, SEM and nanosizer. The particles (4) were spherical and monodisperse with an average diameter of 316 nm. To mimic biological reduction in cancer cells, drug release studies at pH 5.5 revealed that chemical reduction of (4) with $NaBH_4$ gave $[Co^{2+}(Cbl)]$ and significantly induced release of the Pt drug. The results suggested that Cbl not only could serve as a targeting molecule but also a gatekeeper to prevent the drug release before reaching the targeted cells.

Department:	Chemistry	Student's Signature	.....
Field of Study:	Chemistry	Advisor's Signature	.....
Academic Year:	2015	Co-Advisor's Signature	.....

ACKNOWLEDGEMENTS

This research project would not have been possible without the help of many people in so many ways. It was the period of goodtime as I receive the generous assistance. At the same time, it was very hard time that I had to pay all of my perseverance, motivation, and attention to execute this project. At this time, I am so proud that I have completed my Master degree.

First of all, I would like to take this opportunity to sincerely appreciate and gratefully acknowledge to my research advisor and co-advisor, Professor Thawatchai Tuntulani and Dr.Pannee Leeladee, for encouraging me in our project. I own my debt of gratitude for giving me the vision and foresight, which inspired me to conceive this project. Without their support, the project would not be succeeded.

It is a genuine pleasure to express my deep sense thank and gratitude to the committee (Assoc.Prof.Dr Vudhichai Parasuk, Dr. Numpon Insin, Dr. Nawaporn Vinayavekhin, and Dr. Chaweewan Sapcharoenkun) and Dr. Piyanuch Wonganan, Faculty of Medicine, for the kindness and enthusiasm suggestion. There are a lot of helpful advices pushing forward me to complete our research.

I am particularly in debited to researcher from National Nanotechnology Center (NANOTEC) for the generous help and co-operation throughout my master degree. I also place on record, my sense of gratitude to Sci spec Co., LTD for ICP-AES analysis. Moreover, I would like to sincerely thank you to Sensor Research Unit (SRU) for allowing me to use tip sonication. Besides, I also wish to extend my faithful thanks to the financial support from The 90th Anniversary of Chulalongkorn University scholarship and Research Assistant scholarship.

In addition, it is my privilege to thank Supramolecular Chemistry Research Unit (SCRU) for the friendship and helping me while I was preparing on the experiments. Thank you for giving me the useful suggestion, which I could utilize it on my work.

Finally, I am extremely thankful to my beloved family who always offer me encouragement, a loving reproach, a place of rest. I could not imagine how I can finish this project without their warmheartness.

CONTENTS

Page

Page

Page

LIST OF TABLES

Page

LIST OF FIGURES

Page

LIST OF SCHEMES

Page

LIST OF ABBREVIATIONS AND SYMBOLS

g	Gram
μg	Microgram
h	Hour
min	minute
mmol	Millimole
M	Molar
mM	Millimolar
mL	Milliliter
nm	Nanometer
cm^{-1}	Reciprocal centrimeters
ppm	Part per million
PSNs	Porous silica nanoparticles
$PSNsNH_2$	Aminated-porous silica nanoparticles
CblPSNs	Cobalamin-grafted porous silica nanoparticles
PSNsCOOH	Carboxyl-porous silica nanoparticles
CblPSNsCOOH	Cobalamin-grafted carboxyl-porous silica nanoparticles
MSNs	Mesoporous silica nanoparticles
AMS	Amorphous silica nanoparticles
CDDP	Cisplatin
DOX	Doxorubicin

Cbl	Cobalamin
FA	Folic acid
DMB	5,6-dimethyl benzimidazole base
HC	Haptocorrin
IF	Gastric intrinsic factor
TCII	Transcobalamin
TCII-R	Transcobalamin receptor
TEOS	Tetraethylorthosilane
APTES	(3-aminopropyl)triethoxysilane
CTAB	Cetyl trimethylammonium bromide
CES	Carboxyethylsilane
PBS	Phosphate buffer solutions
DMSO	Dimethylsulfoxide
THF	Tetrahydrofuran
HCl	Hydrochloric acid
KBr	Potassium bromide
$AgNO_3$	Silver nitrate
AgCl	Silver chloride
$NaBH_4$	Sodium borohydride
MeOH	Methanol
EtOH	Ethanol
DI H_2O	Deionized water
DDS	Drug delivery system
SEM	Scanning Electron Microscopy

DLS	Dynamic Light Scattering
ICP-AES	Inductively Coupled Plasma-Atomic Emission Spectroscopy
FT-IR	Fourier transform infrared spectroscopy
XRD	X-ray diffraction patterns
ESI-MS	Electrospray ionization-mass spectrometry
UV-vis	UV-visible spectroscopy
DR-UV	Diffuse reflectance UV-visible spectroscopy

CHAPTER I

INTRODUCTION

1.1 Background and significance

Chemotherapy is widely used in cancer treatments. In this process, the drug would interact with the active sites of tumor, causing the cell death. Unfortunately, there are some drawbacks. For instance, the treatment showed harmful effects to the healthy cells [1]. The patients who take anticancer drugs can suffer from the side effects as well as drug resistance [2] since most of the drug administrated does not reach the targeted cells and cannot maintain the drug level at the active sites [3]. To overcome these drawbacks, drug delivery system has been developed in order to carry and transport drugs to cancer cells selectively and efficiently. Drug delivery system consists of three components, which are anticancer agent, drug vehicle, and targeting molecule. The targeted system is expected to enhance the potential of drugs and reduce those side effects. In our study, cisplatin (CDDP) is considered to use as an anticancer drug model due to its high performance for therapeutic effects. The drug will be encapsulated in a drug carrier to enhance its bioavailability and prevent the drug interactions. Such a drug carrier includes porous silica nanoparticles (PSNs). These nanoparticles have been utilized as drug vehicle owing to its large pore volume, large surface area, easy functionalization, biocompatibility and stability. [4, 5] However, the nanoparticles still lack of specificity. To increase the selectivity of the system, a specific molecule is needed to deliver the drug to cancer cells by binding selectively with the receptor. An example of such receptors is transcobalamin receptors or TCll-R which are overexpressed on the surface of many types of cancer cells, including ovarian cancer, skin cancer, and brain tumor. [6] Hence, cobalamin (Cbl) or vitamin B_{12} can potentially serve as a targeting molecule to bind TCII-R selectively and enhance the cell uptake efficiency of the system by receptor-mediated endocytosis. In addition, cobalamin might be simply fabricated onto nanoparticles via noncovalent interaction through the cobalt center. Moreover, the large molecule of Cbl could act as a

gatekeeper for reducing the release rate of cisplatin from the drug carrier during the transportation [7].

Herein, we aim to develop a novel drug delivery system for targeted therapy. Our system design consists of PSNs as drug carrier, Cbl as targeting molecule, and cisplatin as anticancer drug model. Our strategy is to prepare Cbl-conjugated PSNs (CblPSNs) and to incorporate cisplatin into CblPSNs by simple coordinate covalent bonds. The modified particles are expected to improve the specificity and efficiency of drug system.

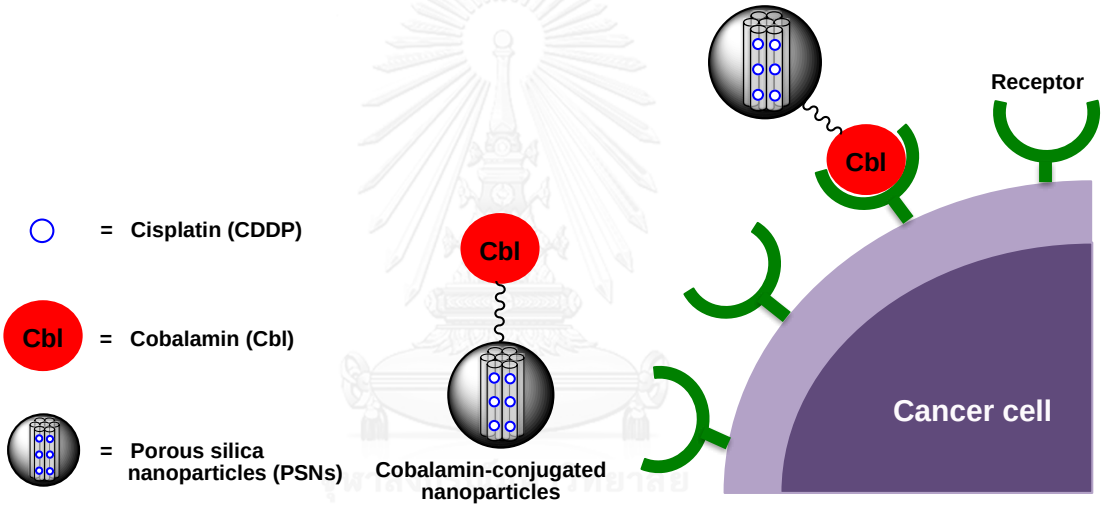

Figure 1.1 CDDP@CblPSNs as drug delivery system for cancer cells (Adapted from Ref.[8])

1.2 Drug delivery system (DDS)

Drug delivery system (DDS) is a construction that improves the introduction of the drug molecules into our body. This system can increase the efficacy of drug, reduce the side effects, and control the rate time. The process of DDS consists of 3 steps. Firstly, the therapeutic agent is loaded into the drug vehicle. Then, the product will be delivered to the cell and the drug will be released. Finally, the drug will be subsequently transported to the site of action [9].

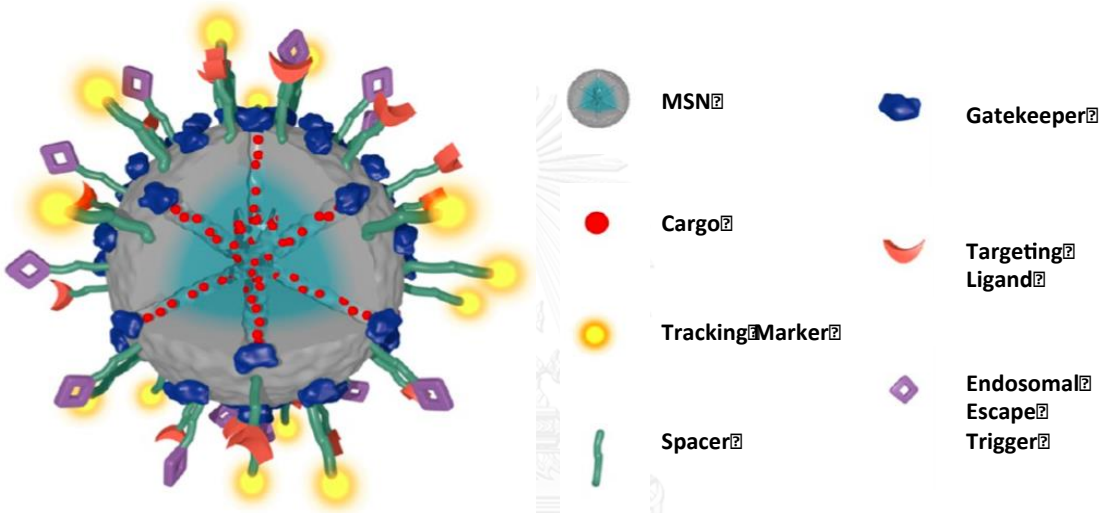

Figure 1.2 The illustration of a multifunction on drug delivery system cells (Adapted from Ref.[7]).

Drug delivery systems have been extensively studied especially for cancer treatment [10]. Typically, a delivery system composes of two major components; therapeutic agent and drug carrier. It could be internalized into cell via oral ingestion, intravascular injection, and blood circulation [11]. However, most of the drugs lack of specificity and are not able to reach the targeted cell. The result is that the system cannot maintain the drug level at the active sites due to the fluctuation in circulation. [3, 12]

To overcome these problems, the multifunction of drug delivery vehicles has been developed to increase the selectivity and potential of drug systems (Figure 1.2).

The examples of modifying drug vehicle include the functionalization of drug carrier to increase the selectivity to targeted cells, the investigation of gatekeepers for controlling the release rate of drug in cargo, and the drug encapsulation by biomolecule to increase the biocompatibility [7]. In 2009, Verraedt et al. synthesized the chlorhexidine loaded in amorphous microporous silica (AMS) as drug delivery system. Their goal was to evaluate the potential of the system for achieving controlled release of chlorhexidine. They found that this system released chlorhexidine in a controlled pathway, which could improve the rate time of the drug [13].

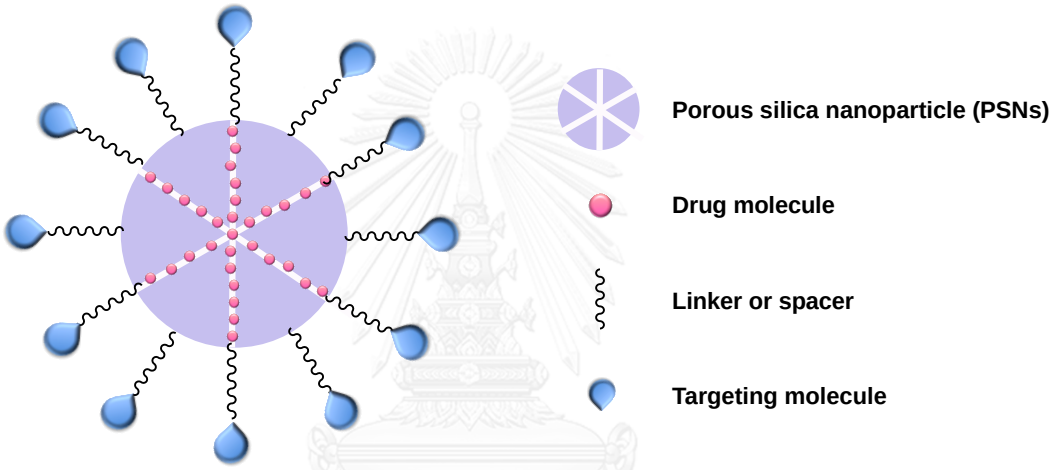

Figure 1.3 Targeted drug delivery system (Adapted from Ref.[7])

Targeted drug delivery is a kind of smart DDS that could specifically transport the medical compound into the tissue of interest (Figure 1.3) [14]. This system is composed of targeting molecules for specific internalization of drug to the active site via nanoparticle-mediated drug delivery (Figure 1.4) [7]. The benefits are that the drug would extremely affect only the malignant cells and reduce the harmful effects to normal cells. Furthermore, it is preferred over the conventional DDS because of several advantages. For example, the non-immunogenic targeting molecule could increase the biocompatibility of the system, which can prolong the lifetime of drug in blood stream. The hydrophobic molecule could improve the solubility of the drug in body fluid. Most of the targeting molecules also have a high specificity pharmaceutical index, which requires only small portion for administration [14-16].

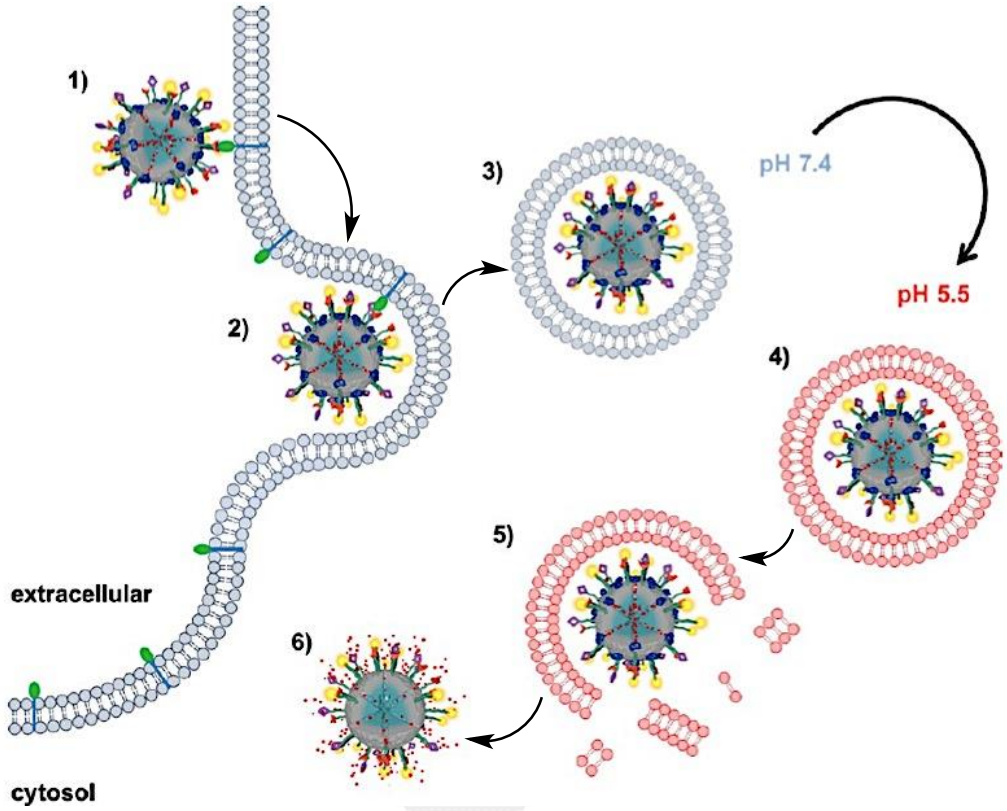

Figure 1.4 Nanoparticle-mediated drug delivery cells (Adapted from Ref.[7]).

In 2010, Zhu et al. synthesized the targeted anticancer drug delivery system based-on folated conjugated (FA) rattle-type Fe_3O_4@SiO_2 hollow mesoporous sphere, combining magnetic targeting and using doxorubicin (DOX) as a model drug (DOX-loaded Fe_3O_4@SiO_2-FA) (Figure 1.5). They found that the DOX-loaded Fe_3O_4@SiO_2-FA was injected by HeLa cells via receptor-mediated endocytosis, which was different from the particle without folated conjugation. The cell uptake efficiency was determined by confocal laser scanning microscopy. The result showed that HeLa cells could take up more DOX-loaded Fe_3O_4@SiO_2-FA than DOX-loaded Fe_3O_4@SiO_2. Besides, both types of particles exhibited the similar biocompatibility to cells. Zhu et al. confirmed that FA grafting facilitate cell uptake of DOX-loaded Fe_3O_4@SiO_2 by HeLa cell [17].

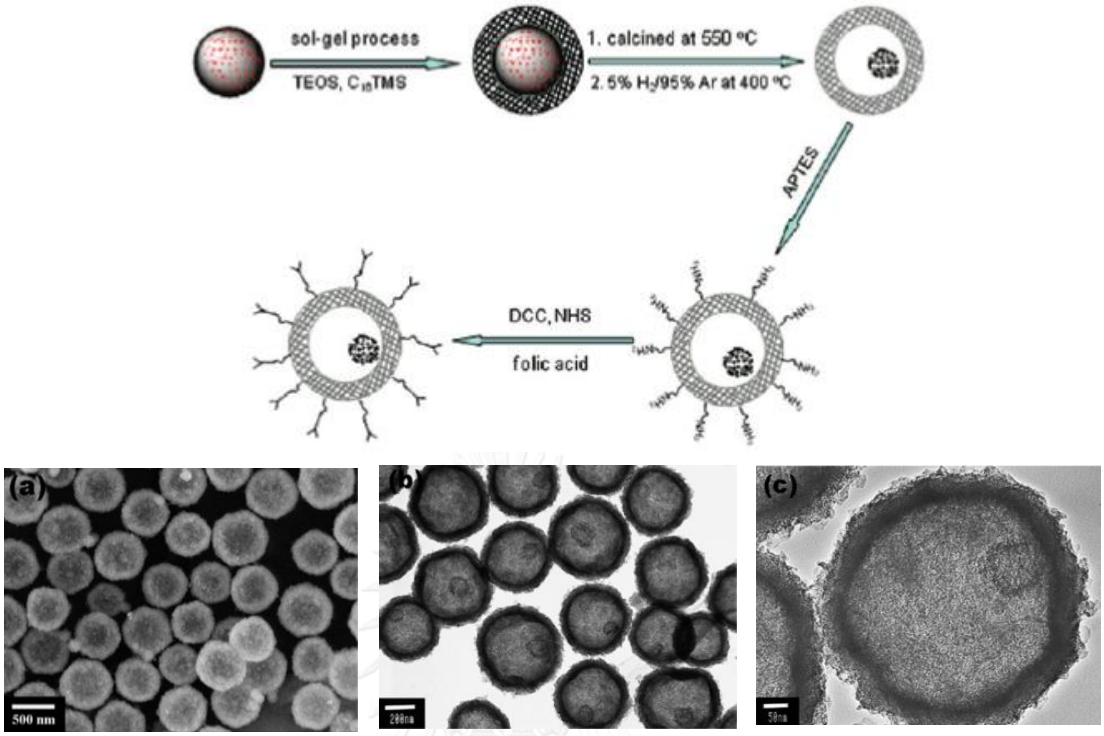

Figure 1.5 The preparation of Fe_3O_4@SiO_2-FA and (a) SEM image of Fe_3O_4@SiO_2, (b) TEM image of Fe_3O_4@SiO_2, and (c) high magnification of TEM for shell thickness (Adapted from Ref.[17]).

In the same year, Tao et al. synthesized platinum drug-loaded mesoporous silica microparticles (MSMs) using MCM-41 and SBA-15. The cell uptake and cytotoxicity of drug were studied on Jurkat cells (leukemia) (Figure 1.6). They found that both types of mesoporous materials were ingested by endocytosis process. Interestingly, they also reported that drug loaded MCMs exhibited the higher anticancer activity than those of free drug and free particles. Hence, drug-loaded particles could become more selective and valuable by improving the localization [18].

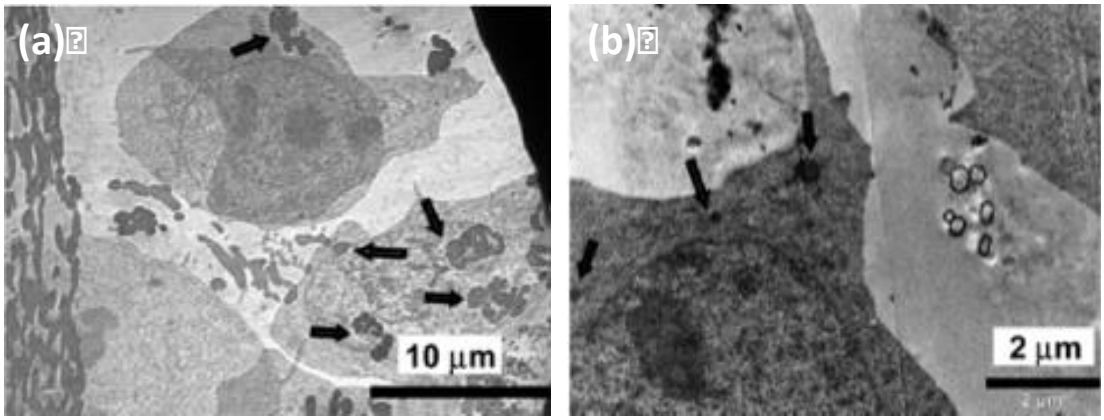

Figure 1.6 TEM images showed the internalizations of (a) SBA-15 and (b) MCM-41 by Jurkat cells (Adapted from Ref.[18]).

1.3 Cisplatin

Cisplatin (Cis-dichlorodiammineplatinum(II), CDDP) is one of the most widely used cytotoxic agent in tumor treatment. It was first synthesized by Michel Reyrone in 1895 (Figure 1.7a) [19]. Cisplatin is a neutral square planar compound which has platinum as a center atom and surrounded by two adjacent non-leaving group ammine ligands and two adjacent chloro leaving group ligands [20, 21]. Cisplatin was first administered to patient in 1971 and was approved to be used in anticancer treatment in 1978 [22].

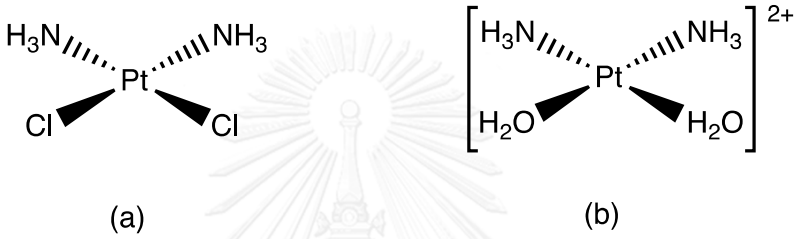

Figure 1.7 The chemical structure of (a) cisplatin and (b) aqua cation species (Adapted from Ref.[23].)

Cisplatin can be entered into the cell by passive transported (Figure 1.8) [22]. The concentration of chloride in cytosol is quite lower than the outer side of cell. As a result, cisplatin tends to form aqua cation species inside the cell (Figure 1.7b), subsequently enter the nucleus and interact with the DNA strand [24, 25]. Because of cation species, it is easy to form a crosslink with N-7 of guanine base, which is the electron richest position (Figure 1.9) [26]. This interaction will interfere the transcription mechanism by kinks the DNA approximately 40° [27]. Unfortunately, cisplatin has the limitations. For example, Pt as a soft metal prefers to bind to soft bases such as sulfur. Once cisplatin bind with high sulfur content biomolecules in blood steam, it will no longer interact with the nitrogen atoms of DNA in nucleus [28]. The good leaving group chloride can also be easily substituted by the other ligands and lead to the decomposition of cisplatin. Furthermore, cisplatin gives the harmful effects to both healthy cells and cancer cells. Therefore, the patients who take this anticancer drug could suffer from its several side effects as well as the drug resistance [29, 30].

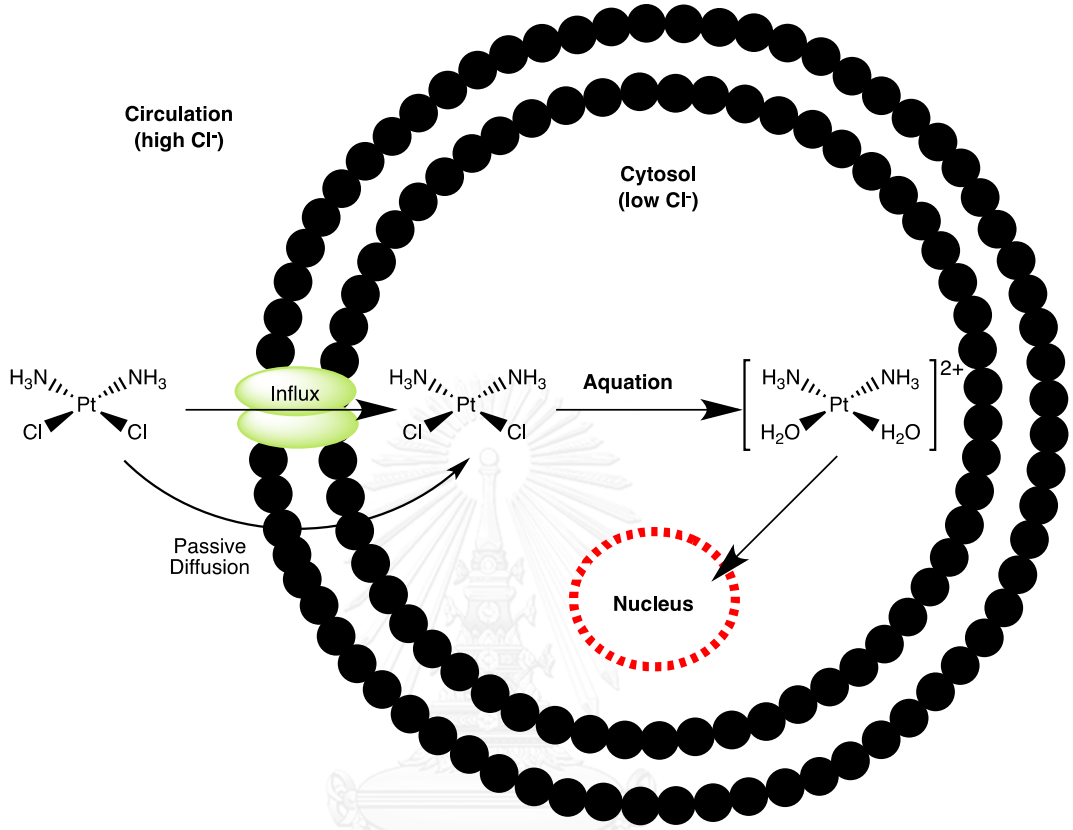

Figure 1.8 The pathway of cisplatin internalized into the cellular (Adapted from Ref.[23])

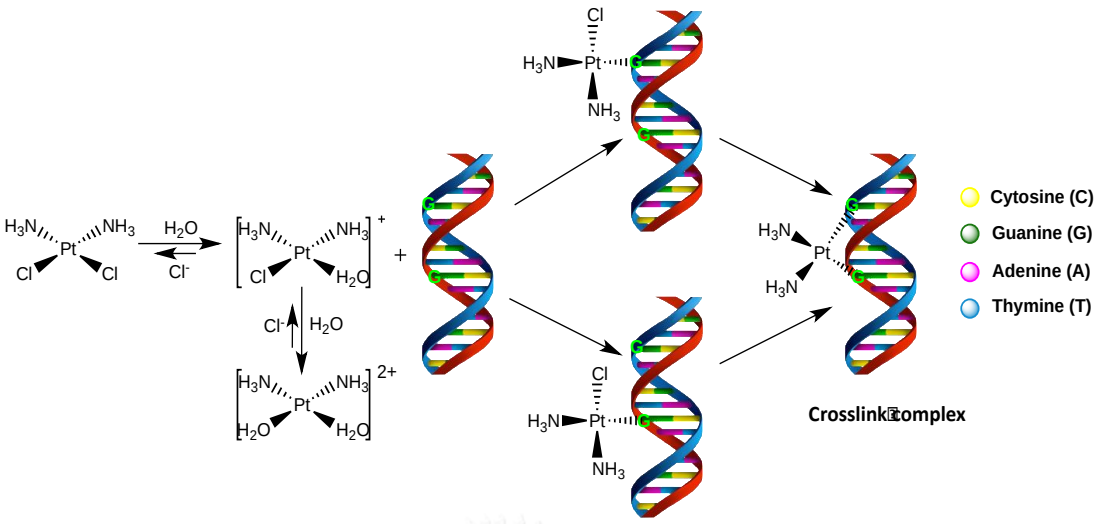

Figure 1.9 The interaction between cisplatin and guanine base of DNA to form crosslink complex. (Adapted from Ref.[31])

There are several approaches to solve these problems such as modifying cisplatin into a new prodrug. Zhang et al. reported novel platinum(IV) complexes with a diverse range of mono-, di-, and mixed-axial carboxylate ligands coupled to the axial positions (Figure 1.10). They found that the complexes of platinum(IV) are more inert than the typical cisplatin (platinum(II)) [32]. This modification led to an increase in the drug stability since the prodrug did not decompose or change into new compounds before reaching the targeted cell. The prodrugs was only active when reduced by bioreduction molecules, which they can be further exploited in drug design without interfering by toxicity [32]. However, they still have some disadvantages such as no selectivity and specificity to targeted cell, and some prodrugs lost their effects after the reduction. Because of these reasons, a number of new systems have been investigated.

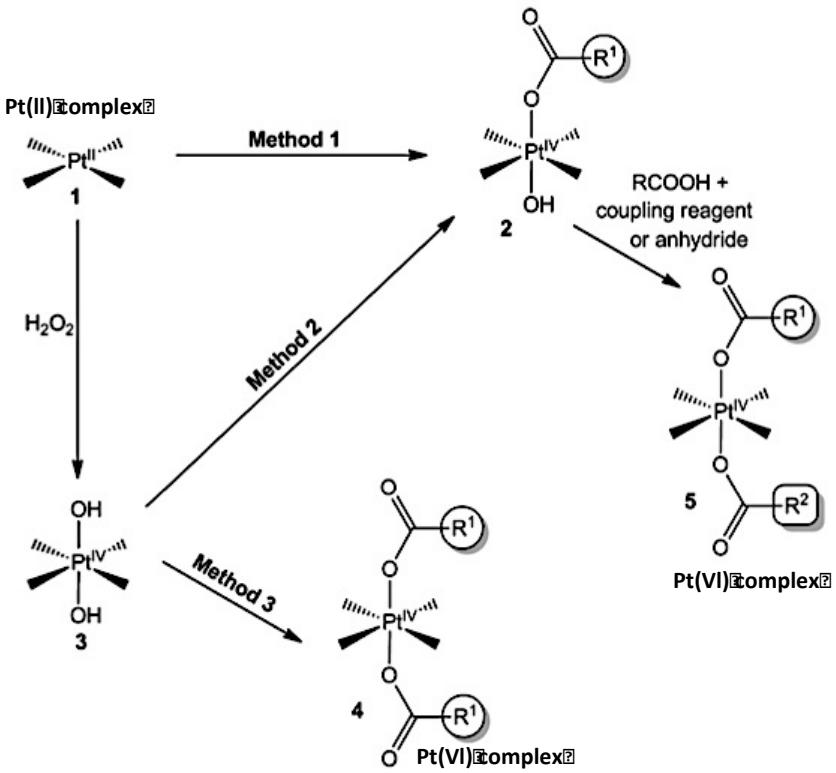

Figure 1.10 Reaction pathway for formation of platinum (IV) complexes. (Adapted from Ref.[32]).

Another approach is to modify cisplatin-like compound by conjugation with specific molecules as a drug carrier. Sanchez et al. described the conjugation of cisplatin and vitamin B_{12} as the general composition of binuclear molecule [{Co}-CN-{Pt}] (Figure 1.11). Vitamin B_{12} was used as a vehicle to deliver drug to cancer cell. The *in vitro* releasing of cisplatin was studied by reducing Co(III) of vitamin B_{12} to Co(II) using *S. enterica* CobA enzyme. They found that the cisplatin was cleaved from vitamin B_{12} after the reduction. As a result, they concluded that [{Co}-CN-{Pt}] might serve as a high stability drug for cancer therapy [33].

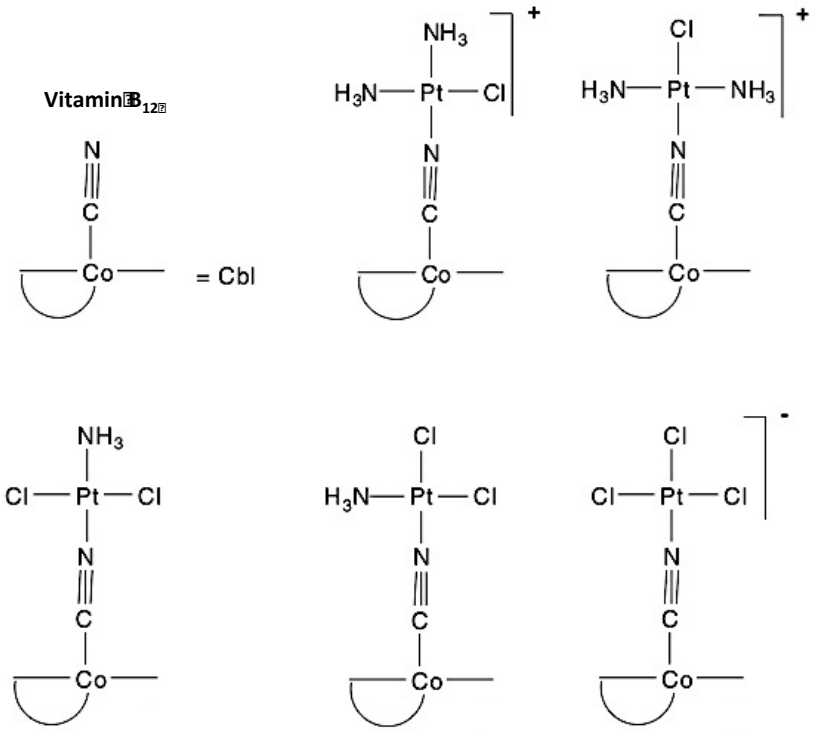

Figure 1.11 The structure of vitamin B_{12} adducts with platinum(II) complexes [{Co}-CN-{Pt}] (Adapted from Ref.[33]).

Nevertheless, the limitation of this process is that the modified drugs are not stable enough to circulate in the blood stream. Some of them showed poor solubility. Thus, loading cisplatin into the drug carrier is an alternative solution. This procedure is one of the best methods because it can increase the stability of cisplatin, decrease the side effects, and enhance the accumulation in tumor. Gu et al. synthesized high-density of carboxyl groups on the surface of mesoporous silica nanocarriers for cisplatin loading (Figure 1.12). They reported that the particles showed high amount of cisplatin loading and could be up taken in to the cell by endocytotic method [34]. It was very interesting that the drug release is acid-dependent. Rosemholm et al. found that at pH 5.5 (cancer cell), 85% of cisplatin was released after 320 h. Meanwhile, at pH 7.4 (blood circulation), the amount was reduced to less than 60%. They concluded that this DDS could minimize the cisplatin leaching in the blood and enable a large amount of intracellular drug releasing [35].

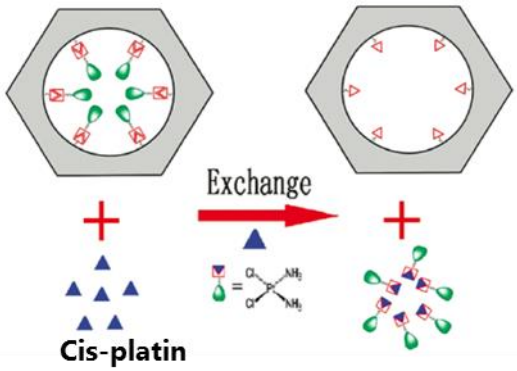

Figure 1.12 The carboxyl group on mesoporous silica nanoparticles with cisplatin loading (Adapted from Ref.[34]).

From all of mentioned reasons, it is particularly important to design the targeted drug delivery system to overcome the drawbacks of cisplatin.

1.4 Porous silica nanoparticles

Porous silica nanoparticles (PSNs) are materials with hundreds of empty channels for absorbing or encapsulating chemical agents. In recent years, PSNs have attracted an attention in various fields including biomedicine, optical sensing, computing system, and electronic field [36]. The reasons are owing to their beneficial structural properties such as high surface area, large pore volume, excellent chemical and thermal stability, narrow particle size distribution, good biocompatibility, and possibility to functionalize on the particle surface [7, 37, 38]. Because of these prominent features, PSNs have been considered as a promising material for various biomedical applications to fight against many kinds of diseases such as diabetes [39, 40], inflammation [41], and cancer [10]. The nanoparticles could be injected into the body via oral, nasal, or intracellular fluid [11]. However, there was no report of using PSNs as nanocarrier in drug delivery system due to the lack of controlling in the particles morphology. Until 2005, the PSNs with the hexagonal porous channel structure were synthesized. This types of PSNs was potentially attractive for controlled releasing delivery application [42]. The reason is that the uniformed structure could exhibit as “zero premature release”, which means that the encapsulated drug will not leak along the transportation [37]. There are a number of PSNs shapes reported in the literatures such as spheres, ellipsoids, rods, and tubes (Figure 1.13) [43, 44]. Our research chose the spherical particles in order to avoid the friction between the particles and circulation vein.

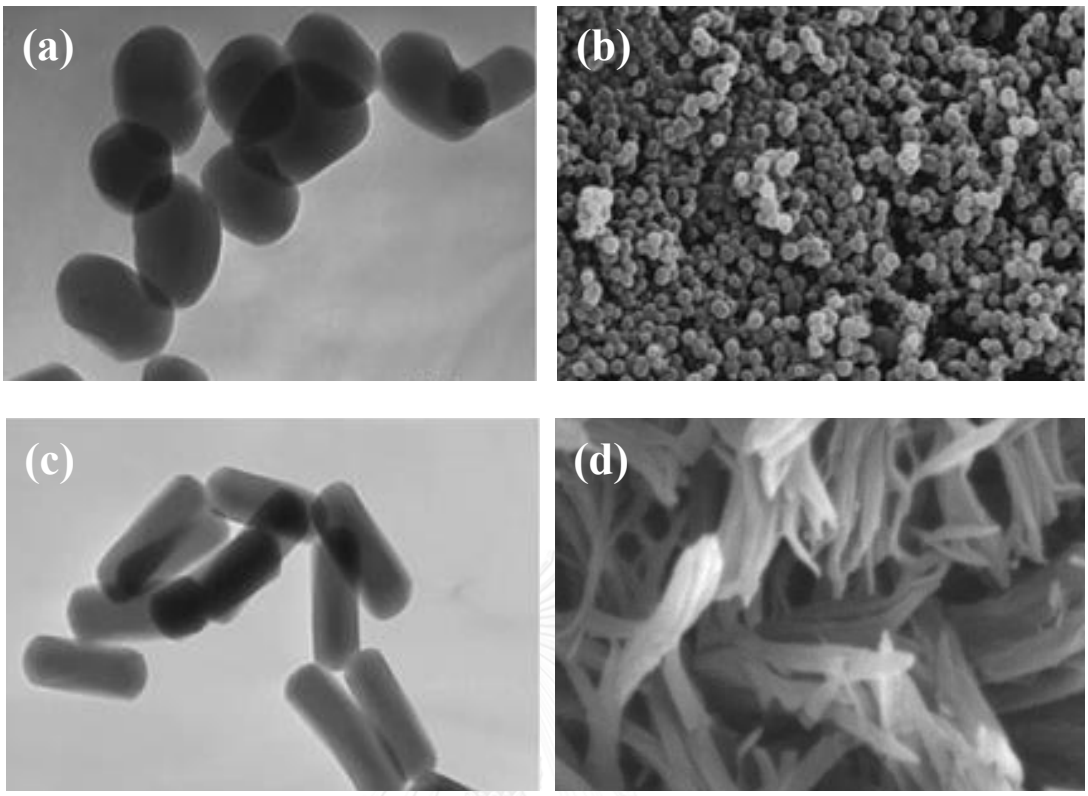

Figure 1.13 The different shapes of porous silica nanoparticles, (a) short rod-shaped particles, (b) sphere-shaped particles, (c) long rod-shaped particles, and (d) tube-shaped particles. (Adapted from Ref.[2])

A number of studies have shown that silica nanoparticles can enhance the stability of delivery system. For example, Li et al. studied the possible mechanisms of cell death induced by free doxorubicin (DOX), free mesoporous silica nanoparticles (MSNs), and doxorubicin loaded in mesoporous silica nanoparticles (DOX@MSNs) incubated in HeLa cell (ovarian cancer cell) (Figure 1.14). From MTT results, free MSNs showed no cytotoxicity to HeLa cells, which could confirm that silica nanoparticles were biocompatible to living cells. However, both free DOX and DOX@MSNs exhibited cytotoxicities and became more significant when increasing the drug concentration and incubation times. Interestingly, after 4 h of incubation, cytotoxicity of DOX@MSNs remained higher than free DOX. They also treated DOX and DOX@MSNs to 4T1 and MCF-7 (two types of breast cancer cells) and found that the results were similar to those treated with HeLa cells. Therefore, they suggested that DOX@MSNs remained

the high potential among different cancer cells due to the MSNs-mediated endocytosis and the sustained intracellular release of DOX from MSNs [45].

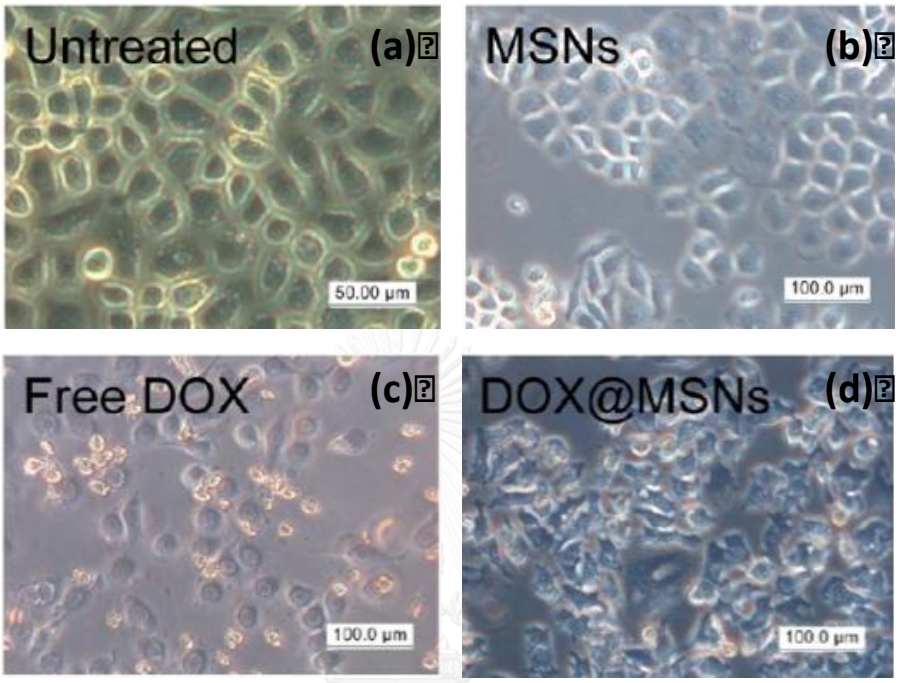

Figure 1.14 The optical images of HeLa cell (a) untreated and treated with (b) MSNs, (c) free DOX, and (d) DOX@MSNs at the same period of time (Adapted from Ref.[45]).

The use of PSNs as drug carriers has been significantly increased over the years. Nonetheless, there are some limitations such as poor solubility, rapid metabolization excretion of the drug, and lack of selectivity of PSNs to the targeted cells. The strategy to improve the targeted transportation is to modify the surface of PSNs, which could be achieved by co-condensation (one-pot synthesis) and grafting (post-synthesis modification), and imprint coating [46-48]. The biocompatibility of PSNs has been studied on the viability and proliferation of various mammals. The internalization of PSNs at concentration less than 100 μg/mL per 10^5 cells showed no effect in growth rates of cells [49, 50]. The efficiency of cellular up taking PSNs depends on particle size and interaction of drug. The particle size should be in range of sub micron. The surface of particles is desirable to interact with the drug compound in order to achieve the large capacity. PSNs exhibit all high performance properties, which could be

adjusted for intracellular controlled releasing. A number of studies have demonstrated that PSNs are capable of *in vitro* endocytosis by various mammal cells such as cancers (HeLa, NIH-OVCAR-3, PANC-1, 3TL3) [50-55]. It is noted that grafting particles with the specific ligand can enhance the efficacy of cellular uptake by receptor-mediated endocytosis [56]. Pinhassi et al. synthesized folate conjugated arabinogalactan endosomally cleavable peptide methotrexate (FA-AG-GFLG-MTX) as novel drug delivery system. They determined the uptake efficiency by folate-receptor overexpressing cancer cells compared to folate-receptor lacking counterparts. The various concentration of particles were incubated in two types of cancer cells; CHO-AA8-C5 cells (lack of folate-receptor expression) and CHO-AA8-C5-FR**α** cells (high level of folate-receptor expression). They found that FA-AG-GFLG-MTX was selectively associated by CHO-AA8-C5-FR**α** cells (Figure 1.15). However, the association did not appear in CHO-AA8-C5. They confirmed that the targeting drug delivery system could enhance the selectivity of cell uptake [2].

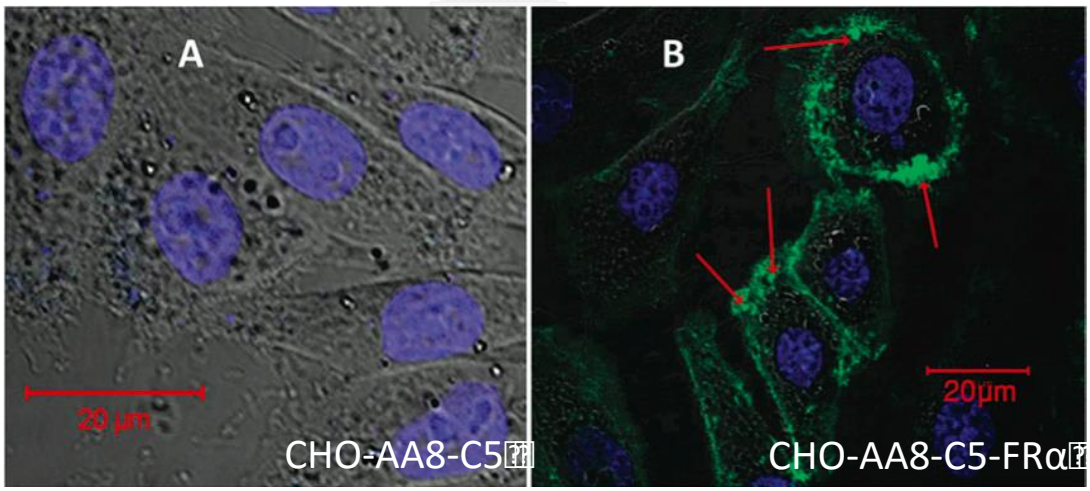

Figure 1.15 The sub cellular localization of the (A) FA-AG-MTX-FITC conjugate in parental C5 and (B) C5-FR **α** (Adapted from Ref.[2]).

1.5 Cobalamin

Cobalamin (vitamin B_{12}, Cbl) is a unique cobalt (Co) complex, which is composed of the highly substituted corrin ring with the Co at the center and the nucleotide appendage with a 5,6-dimethyl benzimidazole base (DMB) (Figure 1.16) [57]. Cbl is necessary for the proliferation and metabolic stability of cells. It participates in the synthesis of thymidine, which support DNA replication of cell division. Thus, the proliferating cells, such as cancer cells demand abnormally high quantities uptake of Cbl [58].

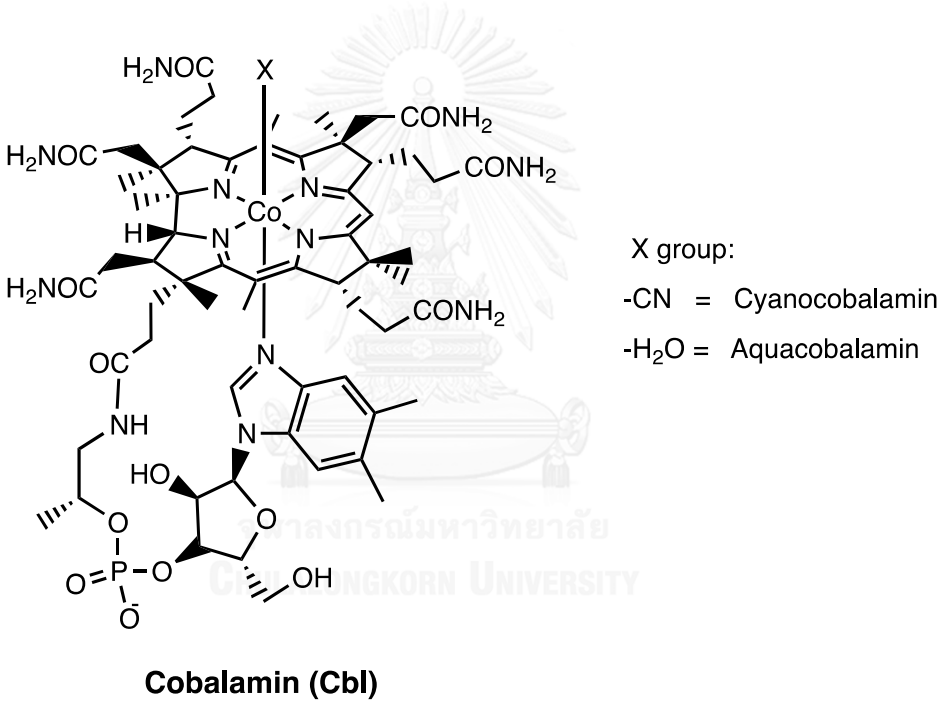

Figure 1.16 The chemical structure of Cobalamin. (Adapted from Ref.[33])

In contrast with the other vitamin molecules, Cbl is remarkably large and cannot be normally taken up by simple diffusion in the intestine [59]. Hence, in mammals the transportation of Cbl is carried out by three proteins namely haptocorrin (HC), gastric intrinsic factor (IF), and transcobalamin (TCll) [60, 61]. The structure properties of human Cbl-binding proteins is shown in Figure 1.17 [60].

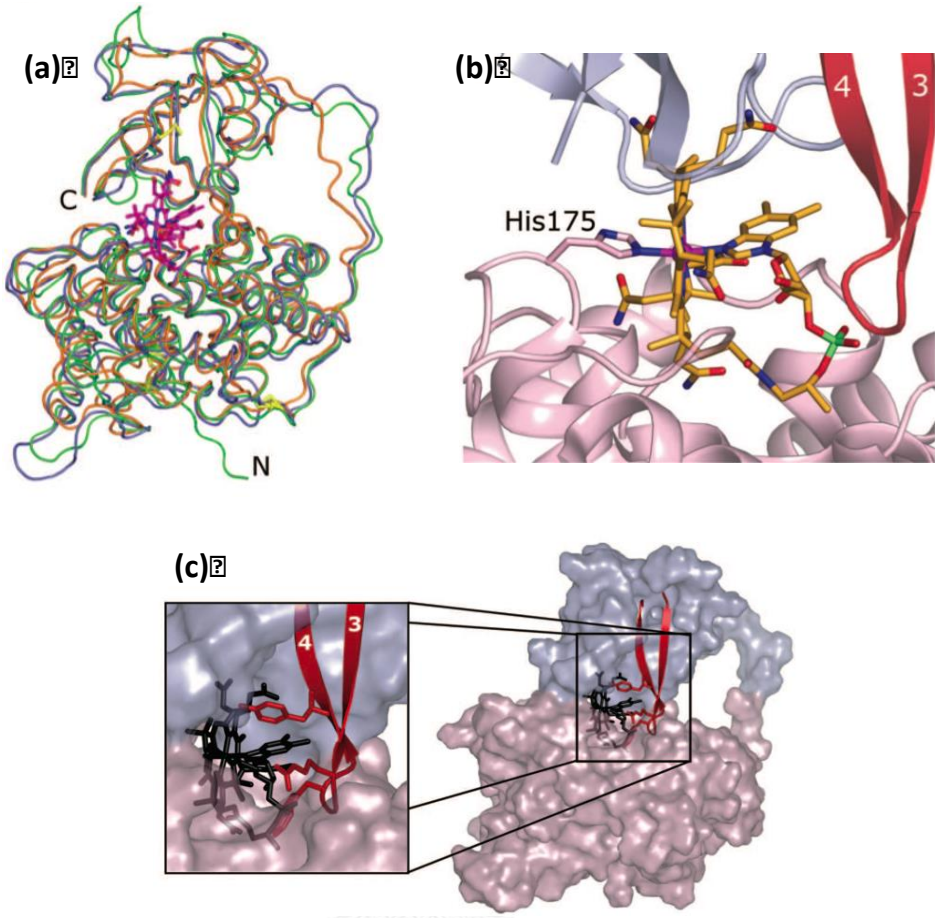

Figure 1.17 Structural properties of human binding proteins. (a) Superposition of the TCII crystal (orange), IF (green), and HC (blue). (b) The Cbl-binding site in TCII. (c) Surface representation of HC model (Adapted from Ref.[60]).

In the stomach, Cbl is initially bound to the HC and form Cbl-HC complex. The HC undergoes proteolytic cleavage into 2 or 3 fragments in the duodenum [60]. Then, Cbl is transferred to IF forming Cbl-IF and subsequently up taken by receptor-mediated endocytosis in the ileum mucosa [62]. In the enterocyte, Cbl is emancipated from IF and transferred to TCll [63, 64]. TCll, the blood cobalamin binding protein, delivers Cbl to the targeted cells via receptor-mediated endocytosis [65]. This pathway has been reported for various cells such as leukemia cells (Figure 1.18). After Cbl internalization, it is converted to co-enzyme (5'-deoxyadenosyl-Cbl and methyl-Cbl) and TCll-receptor will be recycled [66].

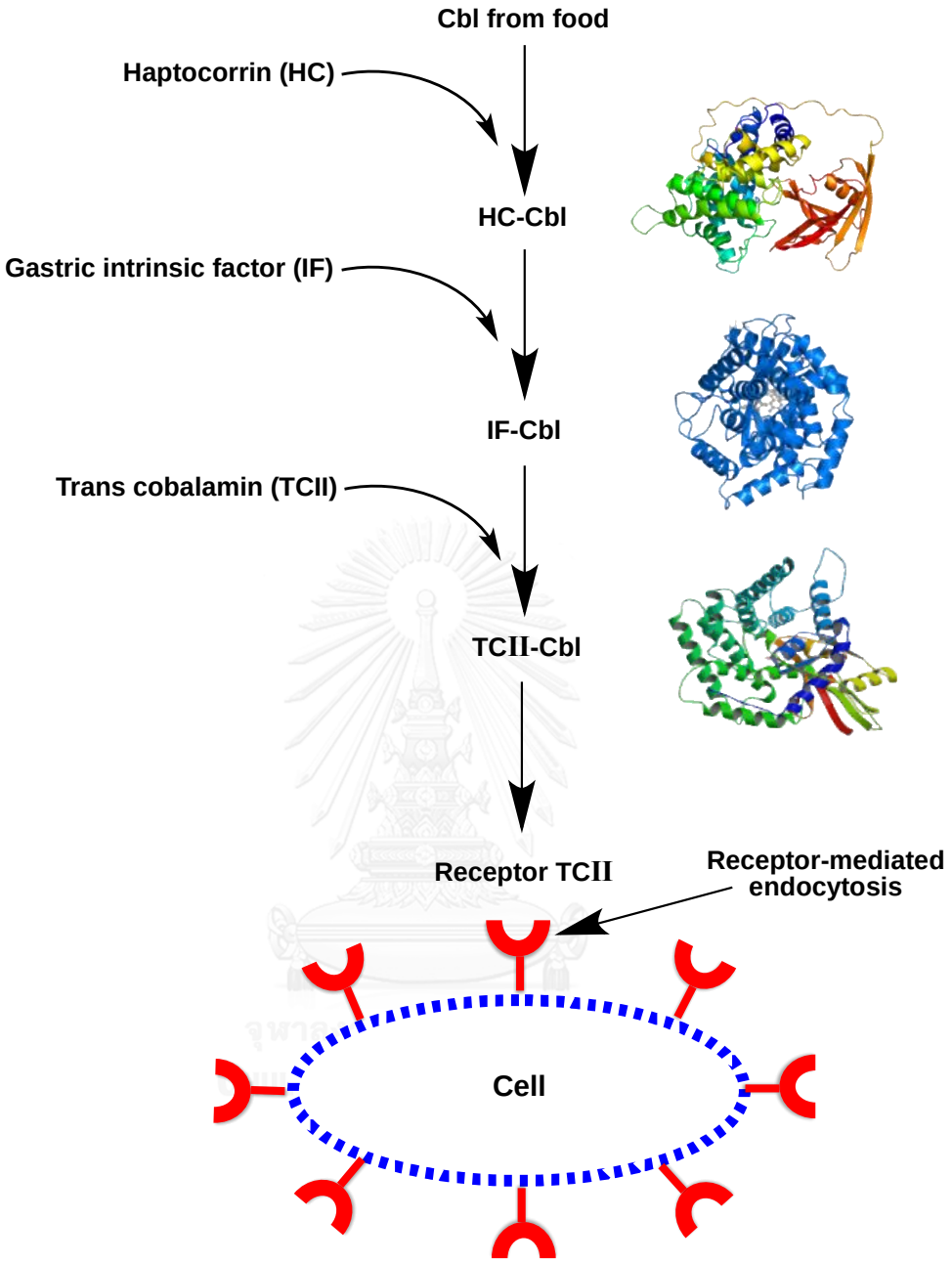

Figure 1.18 The internalization pathway of cobalamin (Cbl) into the cell. (Adapted from Ref.[60])

Consequently, a lot of efforts have been attempted to use Cbl as a targeting molecule due to the attractive features and specific internalization into the cells. Several research groups have described about the transportation of Cbl and the appearance of the Cbl receptor (Figure 1.19). For example, Rhizlane et al. found that HT-29 colon carcinoma expressed the IF receptor in the brush boarder membrane,

which involved receptor-mediated endocytosis of Cbl-IF complex. They also reported that HT-29 cells could synthesize TCll for targeting Cbl in the blood stream. In addition, another colon carcinoma called CaCo2 cells also contains the similar receptor [62]. Sysel et al. and Bauer et al. reported that many types of cancer cells (MCF-7, NIH-OVCAR-3, ACHN, MDS, WI-38, Caov-3, and so on) possessed the protein receptors [67, 68]. According to the previous literatures, Cbl is one of the potential markers for cancer therapy. Hence, Cbl is chosen as the targeting molecule in our drug delivery system for targeted therapy.

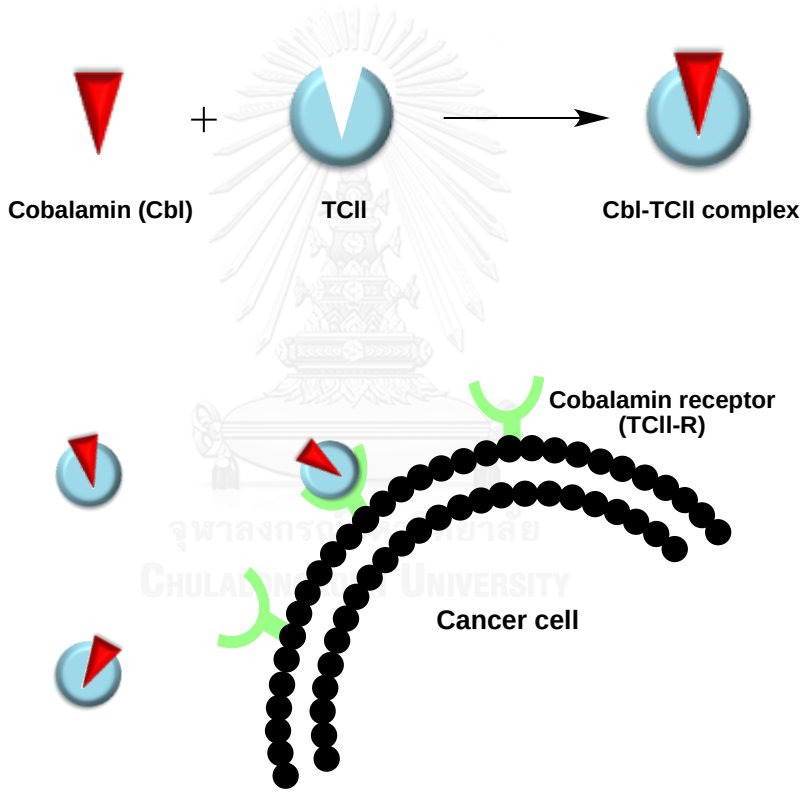

Figure 1.19 The internalization pathway of Cobalamin via receptor-mediated endocytosis. (Adapted from Ref.[65])

In our work, a new drug delivery system is composed of cisplatin (CDDP) as an anticancer agent, porous silica nanoparticles (PSNs) as a drug carrier, and cyanocobalamin (Cbl) as a targeting molecule. We hypothesize that the cobalamin on our novel nanoparticles would bind to the cobalamin-receptor on the cancer cells,

which could improve the uptake efficiency of targeted cells. Moreover, this coordination is expected to protect cisplatin from the undesirable substitution reaction in circulation.

1.6 Research objectives

1. To synthesize and characterize the cobalamin-grafted silica nanoparticles as a delivery system for cisplatin.
2. To determine the cisplatin loading capacity of the synthesized nanoparticles.
3. To study the cisplatin release behavior of the prepared nanoparticles.

1.7 Benefits of this research

Obtained new targeted anticancer drug delivery system based on cobalamin-conjugated porous silica nanoparticles.

CHAPTER II

EXPERIMENTAL

2.1 General procedure

2.1.1 Analytical measurement

Scanning electron microscopy (SEM) performed on a JEOL JSM-7610F. Dynamic light scattering (DLS) was carried out on a Malvern Zetasizer. X-ray diffraction pattern (XRD) was determined by using Cu K-α radiation. Fourier Transform Infrared spectroscopy (FT-IR) was performed on Thermo, Nicolet 6700 FT-IR using KBr pellet in the range of 4000-400 cm^{-1}. UV-visible spectroscopy (UV-vis) was recorded by Varian Cary 50 UV-Vis spectrophotometer. Diffuse reflectance UV-visible spectroscopy (DR-UV) was carried out on Shimadzu, UV-2550 UV-vis spectrophotometer. Inductively coupled plasma atomic emission spectra (ICP-AES) were obtained from a Thermo scientific, iCAP 6500 instrument. Electrospray ionization-mass spectrometry (ESI-MS) was characterized using a Quatto micro API instrument. Nitrogen sorption isotherm was obtained on a BELSORP-mini (SN-154). All micropipettes were bought from Eppendorf.

2.1.2 Materials

All solvents were purchased from Merck as standard analytical grade and were used without further purification. Tetraethylorthosilane (TEOS) and (3-aminopropyl)triethoxysilane (APTES) were bought from Merck. Milli-Q water was achieved from Environmental Analysis Research Unit (EARU). Cetyl trimethylammonium bromide (CTAB) was purchased from Calbiochem. Carboxyethylsilane (CES) was bought from International laboratory USA. Cyanocobalamin (Vitamin B_{12}) and Aquacobalamin (Vitamin B_{12a}) were purchased from TCI. Potassium bromide (KBr) was obtained from Fluka as spectroscopy grade and dried in oven at 100 ^{o}C. Phosphate buffer solutions (PBS) were prepared from sodium hydrogenphosphate (Na_2HPO_4) and sodium dihydrogenphosphate (NaH_2PO_4) in Milli-Q H_2O. Cisplatin (CDDP), an anticancer drug was bought from Sigma Aldrich. The microfilter 0.45 μm was purchased from Membrane solution.

2.2 Preparation of cobalamin-grafted silica nanoparticles (CblPSNs)

2.2.1 Synthesis of porous silica nanoparticles (PSNs)

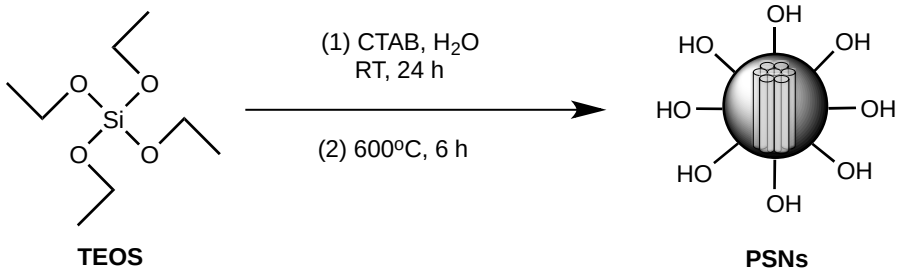

TEOS **PSNs**

The PSNs were prepared according to a published procedure [69]. CTAB (4.00 g, 11.0 mmol) dissolved in DI H_2O (960 mL) was stirred at room temperature for 5 min, after which TEOS (22.6 mL, 11.0 mmol) was added. The solution was continuously stirred for 24 h. The resulting white particles were collected by centrifugation at 10,000 rpm for 30 min. The particles were washed with H_2O and MeOH and were recollected again. Then, the particles were calcined at 600 °C for 6 h to remove CTAB. The white porous materials were obtained. The particles were dried under vacuum for 1 day and kept in a desiccator. The morphology of PSNs was characterized by SEM. The pore size distribution, pore volume, and surface area of particles were determined by nitrogen sorption isotherm. The functional groups of particles were identified by FT-IR spectroscopy. FT-IR: $\boldsymbol{V}$ = 3444 cm^{-1} (OH), 1635 cm^{-1} (OH), 786 cm^{-1} (SiO), 1090 cm^{-1} (SiO), 947 cm^{-1} (SiOH), 831-1260 cm^{-1} (SiO_2)

2.2.2 Synthesis of aminated-porous silica nanoparticles ($PSNsNH_2$)

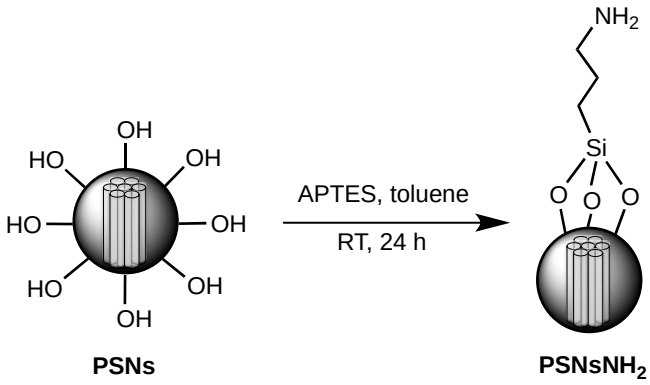

A suspension of PSNs (200 mg) in toluene solvent (80 mL) was added by APTES (0.75 mL). The mixture was stirred at room temperature for 24 h [70]. Then, the resulting product was washed with EtOH (3 times) and collected by centrifugation at 10000 rpm for 20 min. The grafted particles were identified by FT-IR spectroscopy and amino groups on the surface of the particles were confirmed by ninhydrin test. IR: ***V*** = 2981 cm^{-1} (CH_3), 2935 cm^{-1} (CH_2), 3444 cm^{-1} (OH), 1635 cm^{-1} (OH), 786 cm^{-1} (SiO), 1090 cm^{-1} (SiO), 947 cm^{-1} (SiOH), 831-1260 cm^{-1} (SiO_2),

2.2.3 Synthesis of cobalamin-grafted porous silica nanoparticles (CblPSNs)

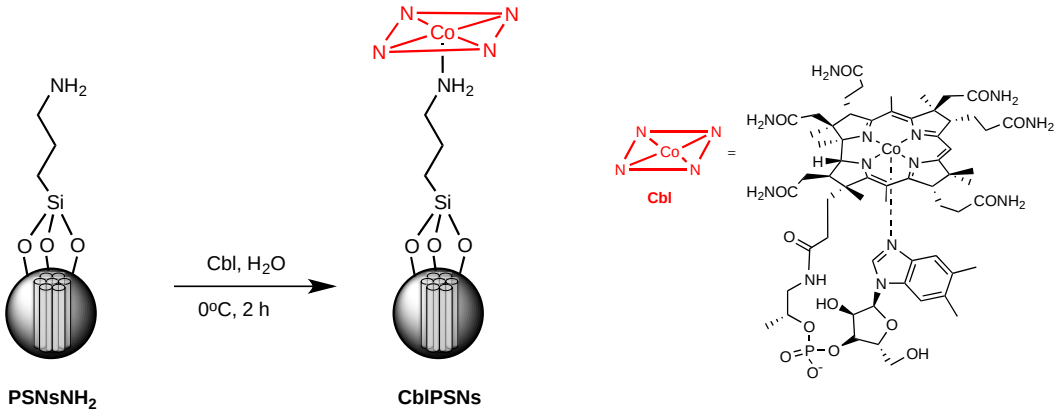

PSNsNH$_2$ **CblPSNs**

Aquacobalamin (0.36 g, 0.22 mmol) was dissolved in DI H_2O (40 mL) and the red solution was stirred at room temperature for 10 min. Then, phosphate buffer solution (PBS) (1.00 mL, 0.1 M pH 7.4) was added into the solution and stirred for 5 min. After that, the solution of $PSNsNH_2$ (200 mg) in H_2O (10 mL) was added to the Cbl solution. The reaction was continuously stirred for 2 h at 0°C. The white nanoparticles became reddish of CblPSNs and were collected by centrifugation at 10,000 rpm at 5°C for 30 min. After that, the particles were washed with H_2O and were dried under vacuum for 12 h. DR-UV spectroscopy was used to confirm the coordination of Cbl on $PSNsNH_2$ in solid state. DR-UV: λ = 348, 547 nm

2.2.4 Incorporated of cisplatin into porous silica nanoparticles

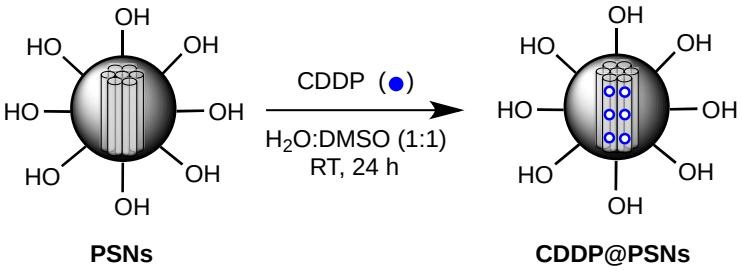

In a typical procedure, a CDDP solution (1000 ppm) was prepared in 1:1 DI H_2O -dimethylsulfoxide (DMSO). Then, PSNs (200 mg) or CblPSNs (200 mg) were added in the CDDP solution and stirred for 24 h at room temperature in dark. The resulting suspensions were centrifuged at 10,000 rpm at 25 ^{o}C for 25 min. The CDDP-loaded particles were washed with DI H_2O and dried in a vacuum for 12 h. [35]. The CDDP solution, supernatant and H_2O washing were collected and the concentration of CDDP was measured by ICP-AES to determined CDDP loading in PSNs. All of the solutions were filtered by 0.45 μm nylon filters before ICP-AES analysis.

2.3 Preparation of cobalamin-grafted cisplatin loaded carboxyl-porous silica nanoparticles (PSNsCOOH)

2.3.1 Synthesis of carboxyl-porous silica nanoparticles (PSNsCOOH)

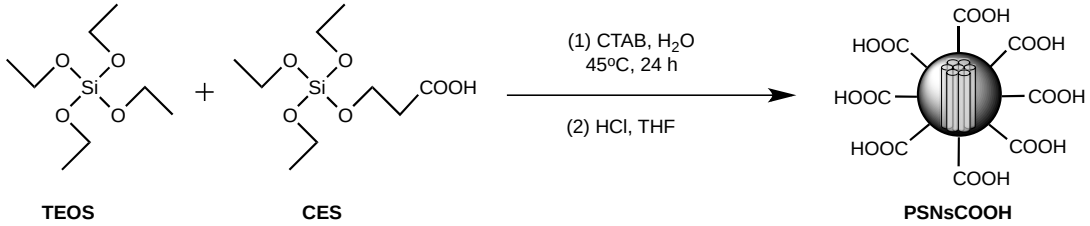

PSNsCOOH was prepared according to a published method [71]. A solution of CTAB (0.75 g, 2.06 mmol) in DI H_2O (250 mL) was stirred at 45°C for 5 min. Into this solution, CES (0.50 mL, 3.38 mmol) was added dropwise and the reaction was stirred for 30 min. TEOS (0.50 mL, 2.47 mmol) in EtOH (5 mL) was then added. The reaction was continuously stirred for 4 h. Then, TEOS (1.50 mL, 7.41 mmol) in EtOH (5 mL) was additionally added in solution and stirred for 1 h. The solution was aged under static condition at 45°C for 24 h. Upon completion, the white powder product was formed in the solution. The particles was collected by centrifugation at 10,000 rpm for 30 min. The obtained particles was refluxed in THF (60.00 mL) with an addition of 2-3 drops of hydrochloric acid (HCl) to remove CTAB template. After that, the particles were washed with DI H_2O and MeOH and were recollected again. The white particles were obtained. The particles were dried under vacuum for 1 day and kept in desiccator.

It should be noted that the same procedure was performed to synthesize PSNsCOOH with different sizes by varying DI H_2O volumes. The three representative nanoparticles with different particle sizes assigned as PSNsCOOH250, PSNsCOOH300, and PSNsCOOH350, respectively, were synthesized with the initial DI H_2O volumes of 250, 300, and 350 mL.

The morphology of PSNsCOOH was characterized by SEM. The hydrated-particle size of PSNsCOOH was analyzed by DLS. The pore size distribution, pore volume, and surface area of particles were determined by nitrogen sorption isotherm.

The functional groups of particles were identified by FT-IR spectroscopy. FT-IR: ***V*** = 1635 cm^{-1} (CO), 1121 cm^{-1} (CO), 2813 cm^{-1} (CH_3), 2852 cm^{-1} (CH_2), 3444 cm^{-1} (OH), 1635 cm^{-1} (OH), 786 cm^{-1} (SiO), 1090 cm^{-1} (SiO), 947 cm^{-1} (SiOH), 831-1260 cm^{-1} (SiO_2)

2.3.2 Incorporation of cisplatin into carboxyl-porous silica nanoparticles

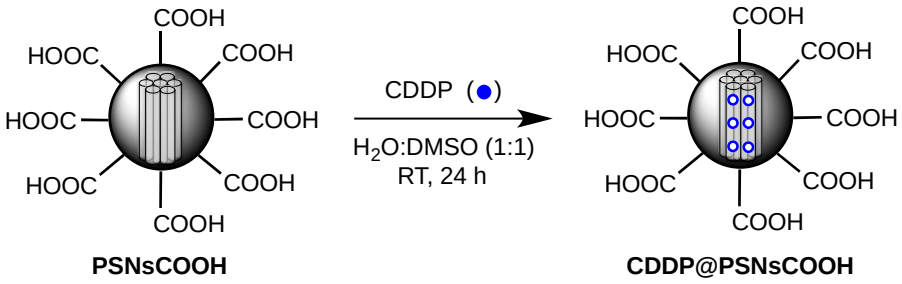

In a typical procedure, CDDP solution (1000 ppm) was prepared in 1:1 DI H_2O - dimethylsulfoxide (DMSO). Then, PSNsCOOH (200 mg) were added in the CDDP solution (50 mL) and stirred for 24 h at room temperature in dark. The resulting suspensions were centrifuged at 10,000 rpm at 25 ^{o}C for 25 min. The CDDP-loaded particles were washed with DI H_2O and dried in a vacuum for 12 h [71].

The CDDP solution, supernatant and H_2O washing were collected and the concentration of CDDP was measured by ICP-AES to determined CDDP loading in PSNsCOOH. All of the solutions were filtered by 0.45 μm nylon filters before ICP-AES analysis.

2.3.3 Synthesis of cobalamin-cisplatin adduct ([Cbl-CDDP]$^{+}$)

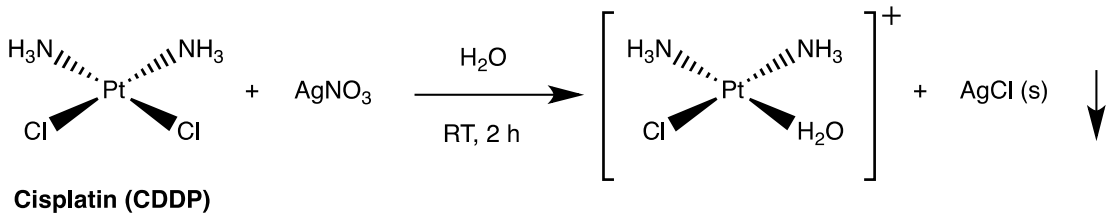

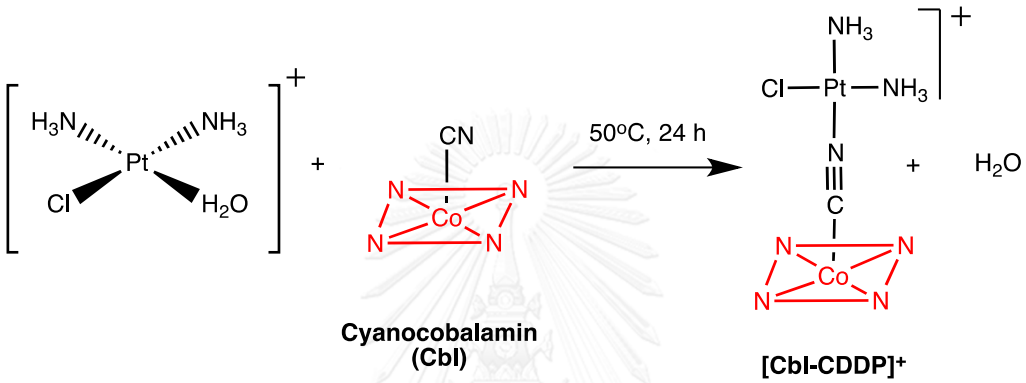

[Cbl-CDDP]$^{+}$ was prepared following a reported procedure [72]. CDDP (0.66 g, 0.22 mmol) and $AgNO_3$ (0.38 g, 0.22 mmol) in DI H_2O (6 mL) were stirred at room temperature for 2 h. The AgCl precipitate was removed from the solvent by centrifugation. Cbl (0.30 g, 0.22 mmol) was then added into the solution and stirred at 50°C for 24 h. The solvent was removed in vacuo. The reddish crude product was obtained. The [Cbl-CDDP]$^{+}$ product was characterized by ESI-MS, IR, and UV-vis spectroscopy. IR: ν = 2199 cm^{-1} (CN); ESI-MS: *m/z* = 1626 $[M]^{+}$; UV-vis: λ = 362 and 549 nm

2.3.4 Synthesis of cobalamin-grafted cisplatin loaded carboxyl-porous silica nanoparticles (CDDP@CblPSNsCOOH)

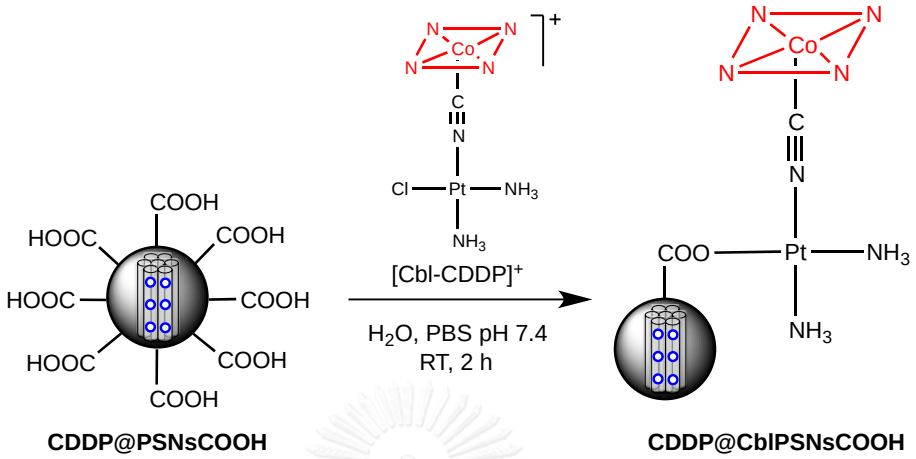

[Cbl-CDDP]$^{+}$ (0.36 g, 0.22 mmol) was dissolved in PBS solution (50 mL, pH 7.4) and stirred at room temperature for 15 min. After that, PSNsCOOH (200 mg) were added to the solution. The reaction was continuously stirred for 2 h. Upon completion, the reddish powder indicating the formation of CDDP@CblPSNsCOOH was observed in the solution. The particles were collected by centrifugation at 10,000 rpm at 5°C for 30 min. After that, the particles were washed with DI H_2O and dried under vacuum overnight. The successful conjugation of Cbl on the particles was demonstrated by chemical reduction of CDDP@CblPSNsCOOH with $NaBH_4$ to yield Co^{2+}(Cbl) and reduced-CDDP@CblPSNsCOOH. UV-vis: λ = 549 nm (Co^{3+}(Cbl)), 470 nm (Co^{2+}(Cbl))

2.3.5 Cisplatin releasing studies

To verify the pH-dependence of drug releasing behavior, the CDDP@PSNsCOOH (0.200 g) were suspended in PBS solution (50 mL, 0.1 M, pH 5.5 or 7.4). The solutions were continuously stirred for 168 h (7 days) at 37°C. Then the supernatant (1.00 mL) was collected at each release time point. The CDDP concentration in supernatant was measured by ICP-AES.

To study the release mechanism of the drug delivery system, 200 mg of CDDP@PSNsCOOH, CDDP@CblPSNsCOOH, or reduced-CDDP@CblPSNsCOOH were suspended in PBS solution (50 mL, 0.1 M, pH 5.5). The solution was continuously stirred for 168 h (7 days) at 37°C. Then supernatant (1.00 mL) was collected at each release time point. The CDDP concentration in supernatant was measured by ICP-AES.

CHAPTER III

RESULTS AND DISCUSSION

3.1 Preparation of cobalamin-grafted porous silica nanoparticles (CblPSNs) and cisplatin loading

Cisplatin is a potent anti-cancer agent. However, it also exhibits toxicity to the normal cells and is unstable in human circulation. Therefore, the main objective of this study is to develop a novel drug delivery system to deliver cisplatin selectively to cancer cells. Our system design composed of cisplatin, porous silica nanoparticles (PSNs) and cobalamin (Cbl), PSNs are employed as a drug carrier. Cbl is used as targeting molecule for enhancing the selectivity of the system. The bonding between PSNs and Cbl is coordination, which could be easily synthesized. Our initial plan to prepare CblPSNs for cisplatin delivery is demonstrated in Scheme 3.1.

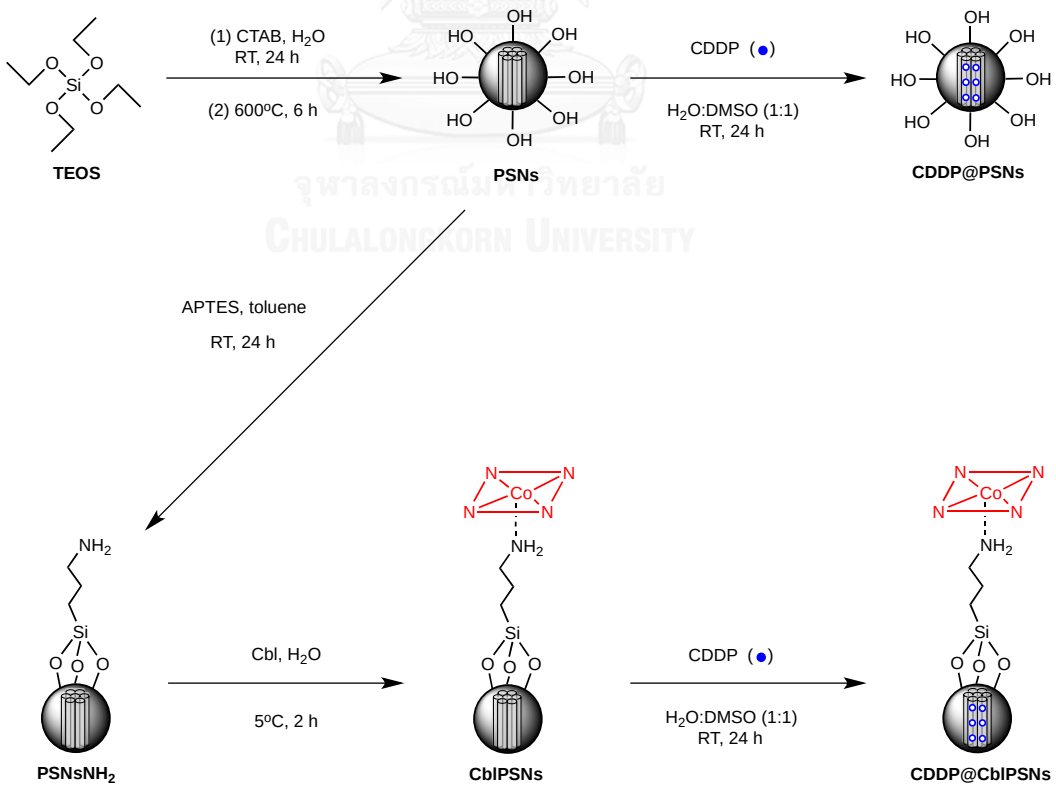

Scheme 3.1 Synthetic pathway of CDDP@CblPSNs

3.1.1 Synthesis and characterization of CblPSNs

The synthesis of PSNs is shown in Scheme 3.1 [69]. These particles were obtained from the polymerization of TEOS in water at room temperature under nitrogen atmosphere. Firstly, CTAB was dissolved in DI H_2O to form a soft micelle template. Then, TEOS was polymerized on the micelle to form the solid particle. After the reaction completed, the particles were collected by centrifugation and the CTAB template was removed by calcination at 600°C for 6 h. The white solid particles were obtained.

The size and morphology of particles were determined by SEM technique. From Figure 3.1b, the PSNs were spherical in shape and monodisperse. The particle size was in range of 130 nm, which is the optimized size to use as a drug carrier [73].

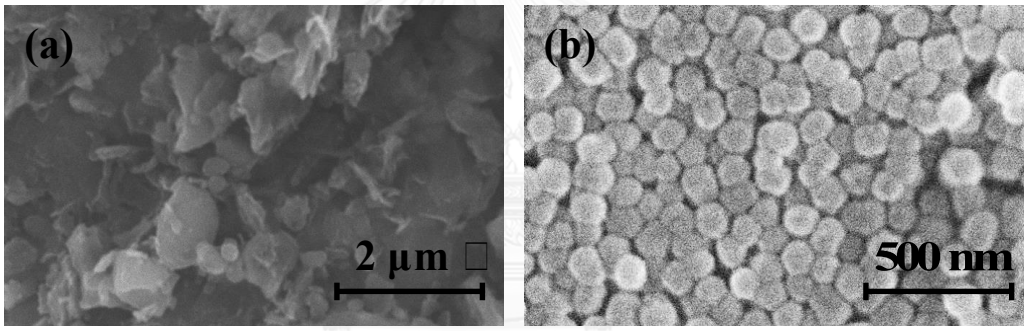

Figure 3.1 SEM images of (a) non-calcined and (b) calcined silica nanoparticles (PSNs).

The functional groups of PSNs were identified by FT-IR spectroscopy. Comparison of IR spectra (Figure 3.2) for non-calcined and calcined nanoparticles also confirms the removal of CTAB template after calcination. The signals of CTAB (2935 and 3050 cm^{-1}) disappear in the calcined PSNs. The silanol functional groups in PSNs were identified around 3440 cm^{-1}, (O-H stretching) and at 1090 cm^{-1} (Si-O stretching) in the IR spectrum [74].

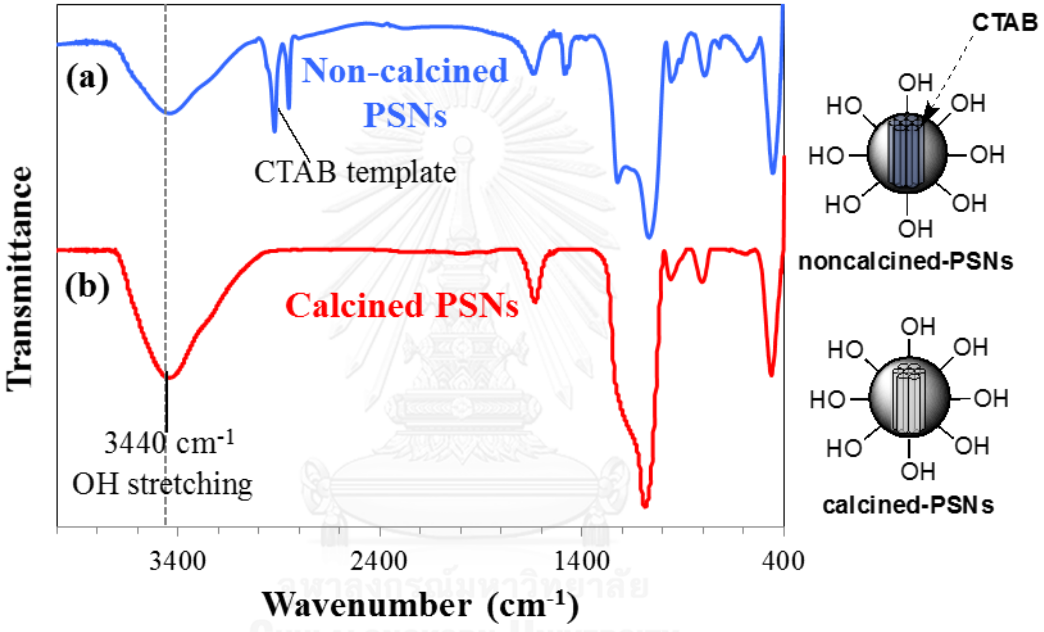

Figure 3.2 The FT-IR spectra of (a) non-calcined PSNs and (b) calcined PSNs.

The pore size, pore volume, and surface area of the particles were determined by nitrogen sorption isotherm. From Figure 3.3, the isotherm can be classified as a type 1 isotherm and the MP-plot (Figure 3.3; inset) revealed the pore size distribution of 1.0 nm, indicative of microporous materials [65]. From Brunauer-Emmett-Teller (BET), the pore volume and specific surface area were 0.429 cm^3g^{-1} and 799.95 m^2g^{-1}, respectively. These characterization data suggested that PSNs were successfully synthesized.

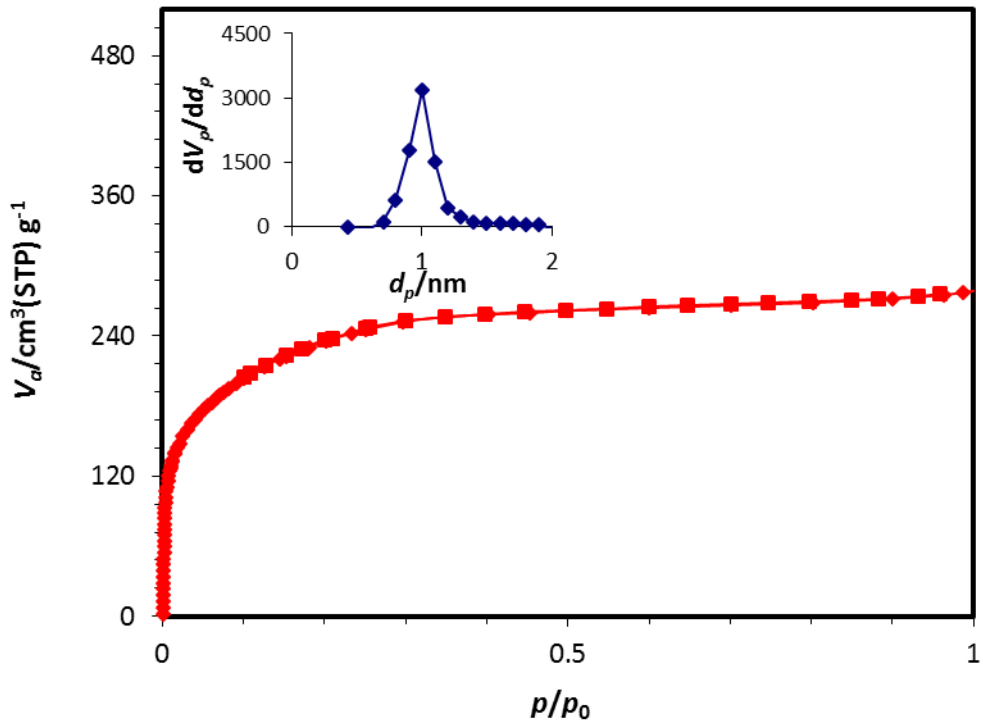

Figure 3.3 The nitrogen sorption isotherm of PSNs. Inset: MP-plot of PSNs

It has been documented that the amino group showed high affinity to Cbl [13]. To incorporate the amino group to PSNs, reaction of APTES and PSNs to obtain $PSNsNH_2$ was carried out. The FT-IR spectrum of $PSNsNH_2$ showed the signals at 2981 and 2935 cm^{-1}, which corresponded to the $–CH_2$ stretching of alkyl chain [13], and suggested the presence of APTES grafting on the nanoparticles (Figure 3.4). The expected signal from N-H stretching was not identified as it was overlapped with that of the O-H stretching from the silanol group.

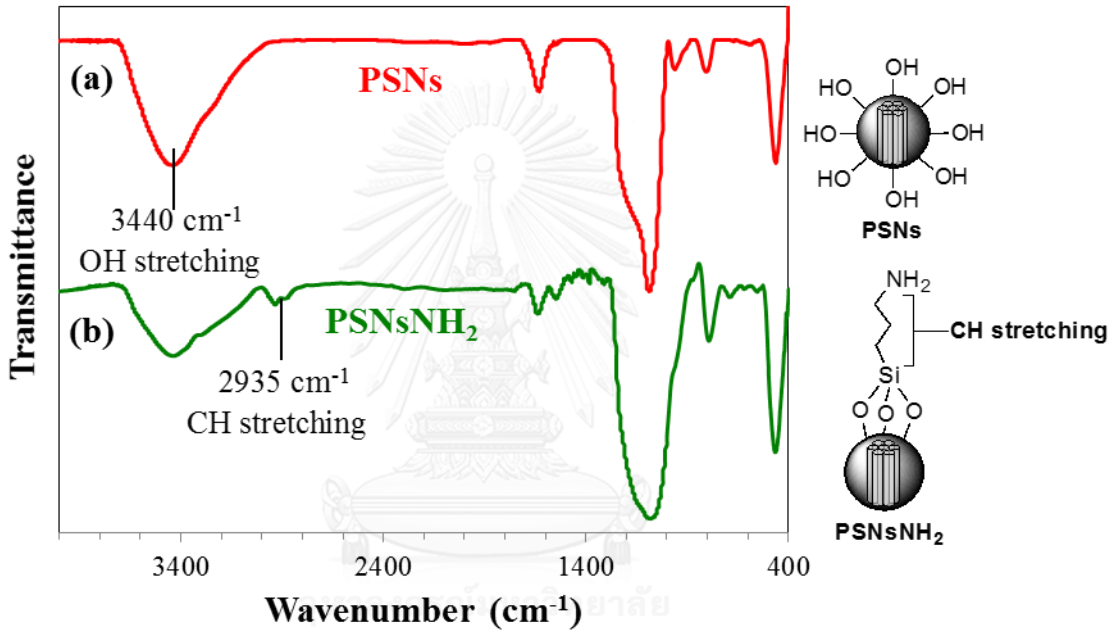

Figure 3.4 The FT-IR spectra of (a) PSNs and (b) $PSNsNH_2$

The amino groups on the particles were confirmed by the ninhydrin test. The experiment was compared between ninhydrin reagent in PSNs (as a control test) and $PSNsNH_2$. It could be seen that the color of ninhydrin did not change in the PSNs solution. However, the reaction between the ninhydrin reagent and the grafted materials resulted in the purple substance shown in Figure 3.5 (Ruhemann's purple), confirming that the amine groups were successfully grafted onto the PSNs (Scheme 3.2) [75].

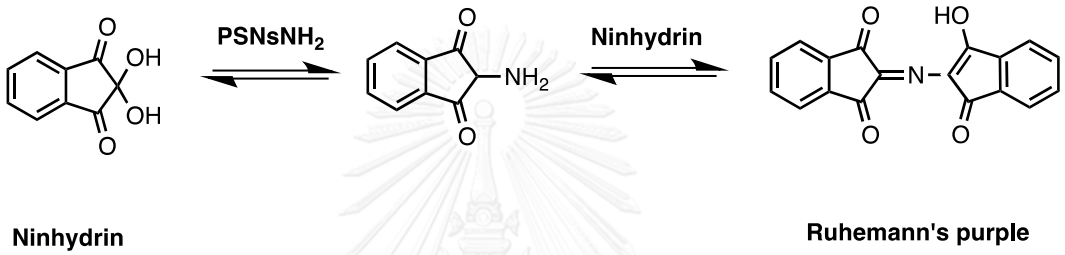

Scheme 3.2 Ninhydrin test of aminated-particles (Adapted from Ref.[75].)

Figure 3.5 The solutions of Ninhydrin test

The Cbl was grafted on the $PSNsNH_2$ to enhance the selectivity of transportation. $PSNsNH_2$ were dispersed in the freshly-prepared solution of aquacobalamin. The white particles of $PSNsNH_2$ turned red, which could suggest that Cbl was grafted on the particles. After the reaction completed, the product were collected by centrifugation. DR-UV spectroscopy was used to confirm the successful conjugation of Cbl on the particles in solid state. From Figure 3.6, the spectrum showed the absorption of cobalamin-grafted particles at 358 nm and 547 nm, which were resembled those of free Cbl [76].

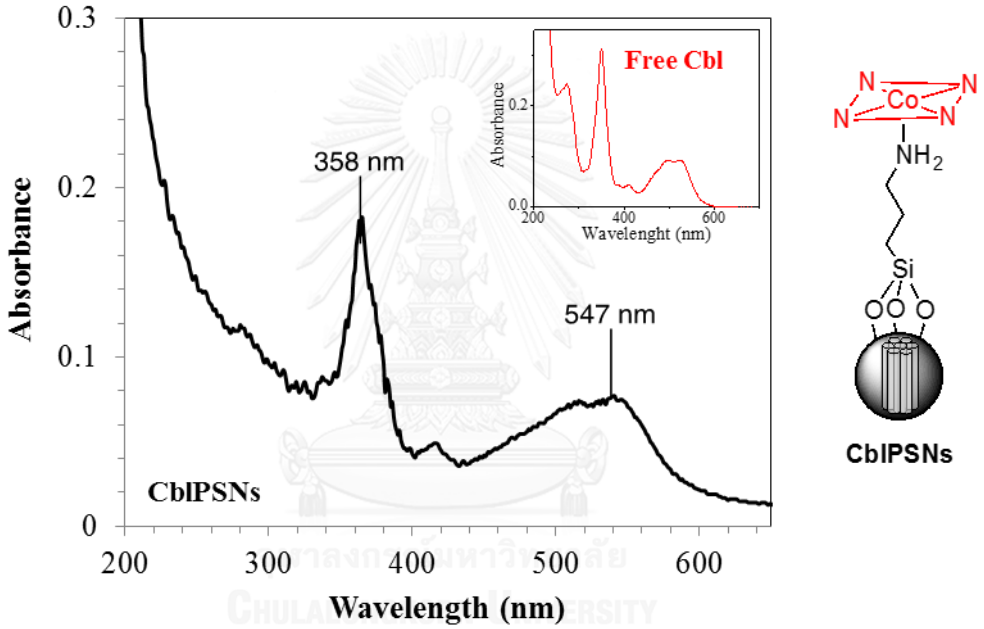

Figure 3.6 The DR-UV spectrum of CblPSNs. Inset: UV-vis spectrum of aquacobalamin.

3.1.2 Cisplatin loading efficiency of PSNs and CblPSNs

Utilization of PSNs and CblPSNs as a drug carrier was examined using cisplatin as a drug model. The amount of cisplatin incorporated in the particles was determined by ICP-AES. Drug loading efficiency was then calculated (Equation 1) [77]. From the results, CblPSNs showed negligible amount of cisplatin loaded in the particles. Our initial hypothesis was that Cbl as a large molecule grafted on the particle surface might inhibit the drug loading. Therefore, we tried to load CDDP to PSNs before Cbl conjugation. However, the loading efficiency was not improved significantly. In fact, the loading efficiency of PSNs was only 7%, possibly due to the low affinity of the silanol groups and cisplatin [35]. Hence, PSNs were not suitable to be the cisplatin carrier in our system. The new design of drug vehicle, PSNsCOOH, was next investigated.

Equation (1):

$$\text{Drug loading efficiency}(\%) = \frac{\text{amount of CDDP incorporated in particles}}{\text{amount of CDDP initially added}} \times 100\%$$

3.2 Synthesis of cobalamin-grafted carboxyl-porous silica nanoparticles (CblPSNsCOOH) and cisplatin loading

According to the lack of cisplatin loading performance of PSNs, the silanol group on the particles was modified the silanol group into the carboxyl group. Our assumption was that the high affinity of carboxyl group could improve the loading efficiency of cisplatin [78]. The synthetic pathway for our new system based on PSNsCOOH is shown in Scheme 3.3.

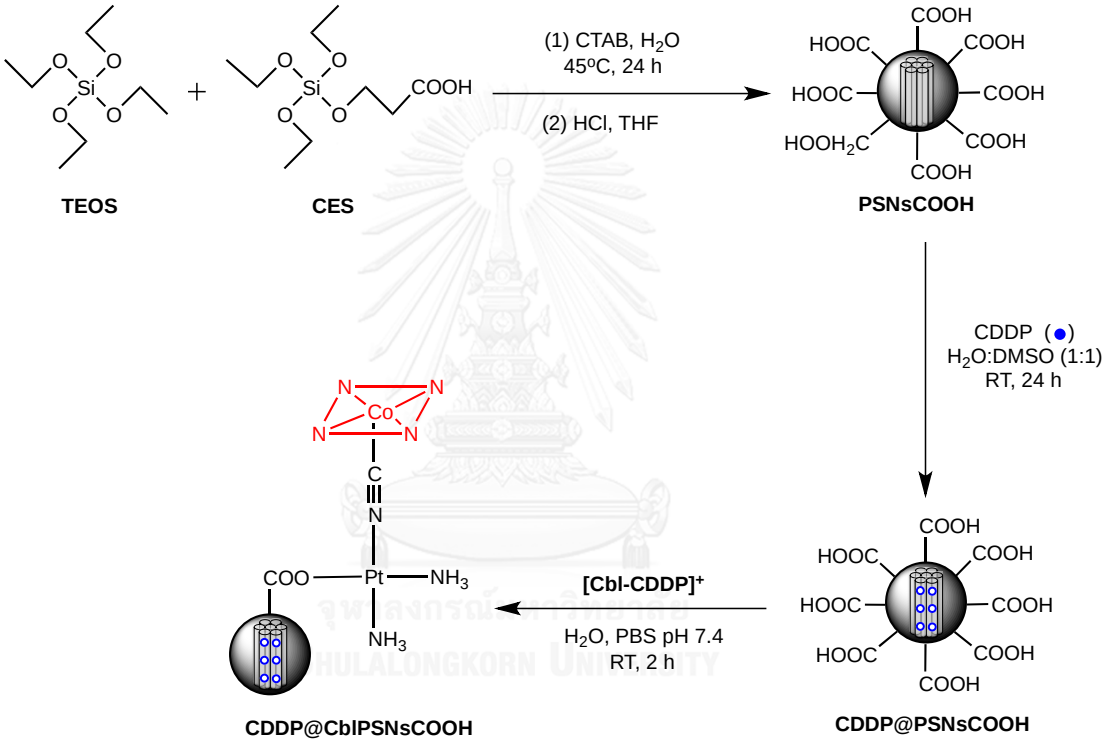

Scheme 3.3 Synthesis of CDDP@CblPSNsCOOH as drug delivery system.

3.2.1 Synthesis and characterization of carboxyl-porous silica nanoparticles (PSNsCOOH)

The PSNsCOOH were synthesized from the co-condensation of TEOS and CES using CTAB as the porous template [35]. The reaction was operated at 45°C under nitrogen atmosphere. CTAB was firstly dissolved in the water to form micelle template. Then, TEOS and CES were co-condensed to form solid particles. The carboxyl group on the particles was not stable in the high temperature. Therefore, the CTAB template was removed by extraction in acid solution instead of calcination. The PSNsCOOH were dispersed in the THF and concentrated HCl was dropped in the solution. The pH of the solution must be less than 5, otherwise the particles would be dissolved due to the protonation of carboxyl group and less amount of particles would be obtained [34]. Finally, the white particles were collected by centrifugation.

It was reported that the concentration of TEOS and CES could affect the particle size. The higher concentration of silicon source led to a larger particle diameter [35]. In our work, we varied the concentration of the silica source by fixing the amount of TEOS and CES in the reaction, but changed the volume of DI H_2O to 250.00, 300.00, and 350.00 mL. The obtained particles were designated as PSNsCOOH250, PSNsCOOH300, and PSNsCOOH350, accordingly.

The morphology of particles was determined by SEM. The representative nanoparticles were dispersed in DI water and were sonicated by tip-sonication. Then, the particle solution was dropped on that the morphology of PSNsCOOH250 and PSNsCOOH300 were both ellipsoidal and spherical particle. In contrast, PSNsCOOH350 were spherical and monodispersed. Dynamic light scattering (DLS) was used to measure the hydrated-particle size in aqueous solution. The diameters of representative nanoparticles were summarized in Table 3.1. The data illustrated that the particle size increased as the water volume decreased, consistent with the published report [35].

In summary, PSNsCOOH350 are in an optimized size and suitable shape for biological tasks. Hereafter, PSNsCOOH350 will be designated as PSNsCOOH and tested as a drug carrier in this research.

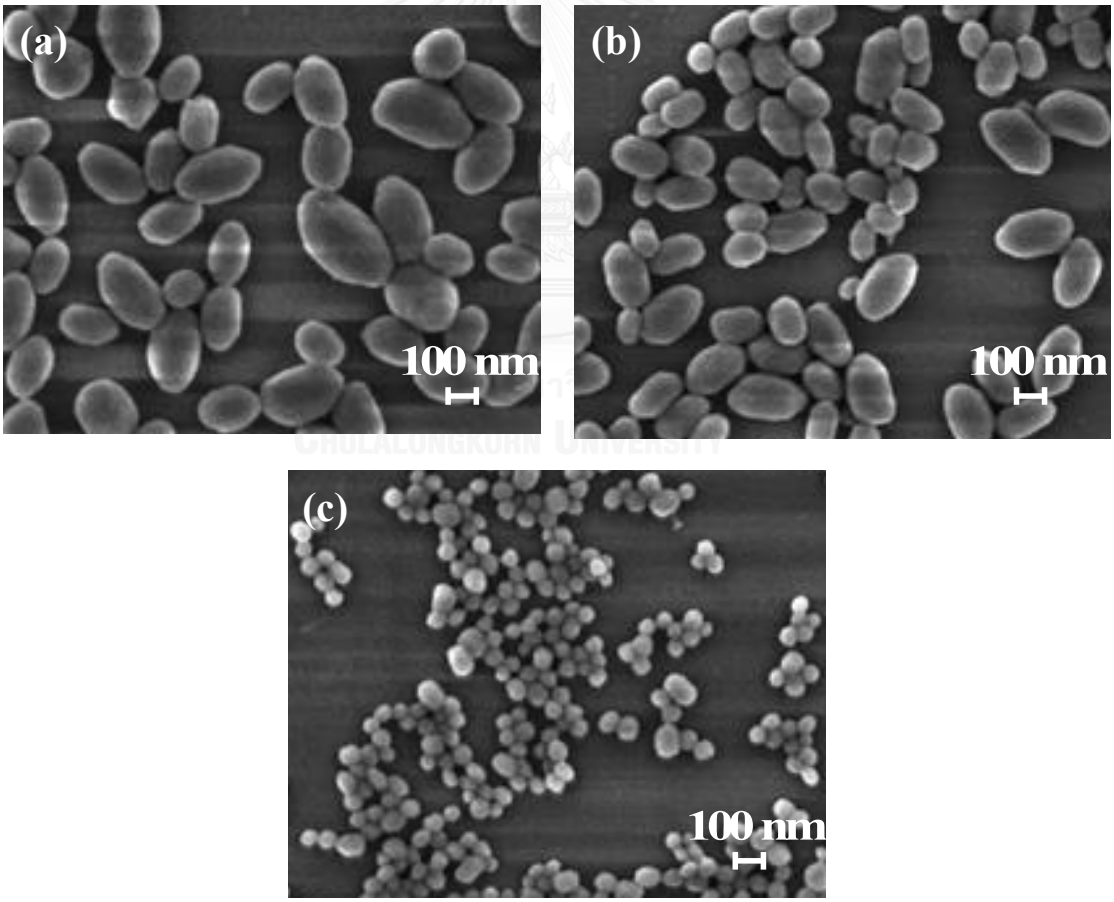

Figure 3.7 The SEM images of (a) PSNsCOOH250, (b) PSNsCOOH300, and (c) PSNsCOOH350.

Table 3.1 The average size of the nanoparticles and grafted-particles determined by DLS technique.

Particle name	Average diameter (nm)
PSNsCOOH250	347 ± 8
PSNsCOOH300	265 ± 8
PSNsCOOH350	173 ± 5

The functional groups on PSNsCOOH were identified by FT-IR spectroscopy. Figure 3.8 showed the absorption peaks at 1635, which attributed to the C=O stretching of terminal carboxylic groups [79, 80]. The result indicated that carboxyl group was successfully introduced to the silica nanoparticles.

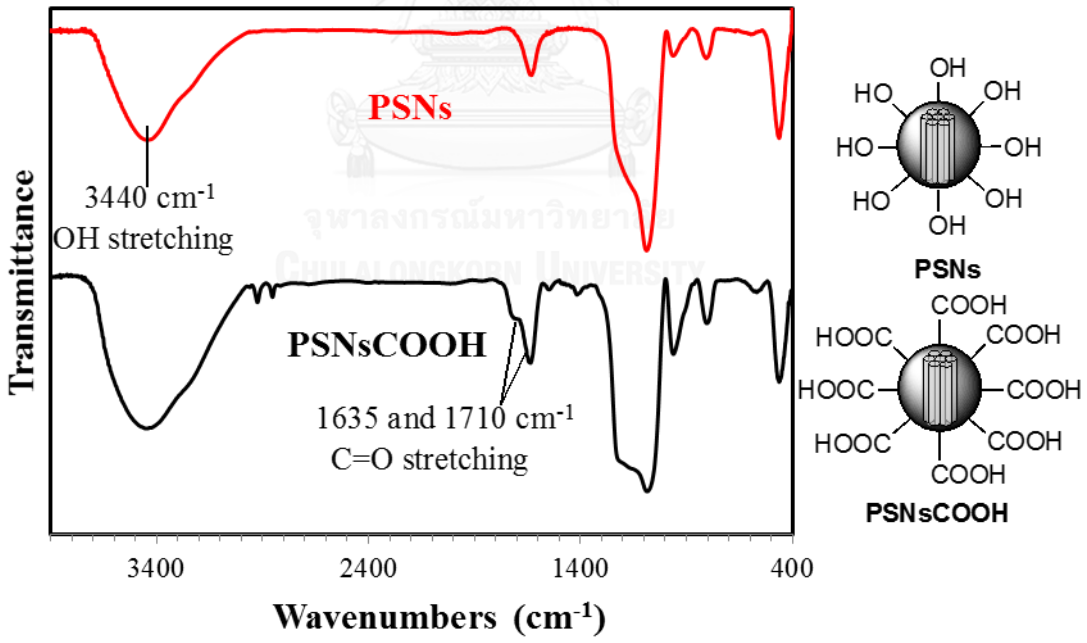

Figure 3.8 The FT-IR spectra of PSNs and PSNsCOOH

The pore size, pore volume, and specific surface area of the particles were investigated by nitrogen sorption isotherm. From figure 3.9, the isotherm could be classified as a Type I isotherm, which is the characteristics of microporous materials [65]. The pore size distribution was calculated from MP-plot (inset picture). It showed a sharp peak at 1 nm, which is in range of micropore [GE]. From BET, the pore volume and specific surface area were 0.637 cm^3g^{-1} and 694.82 m^2g^{-1}, respectively. These particles exhibited the high surface area, which is good for grafting with targeting molecule. They also showed large pore volume for drug storage. These results demonstrated that PSNsCOOH would be a promising drug carrier.

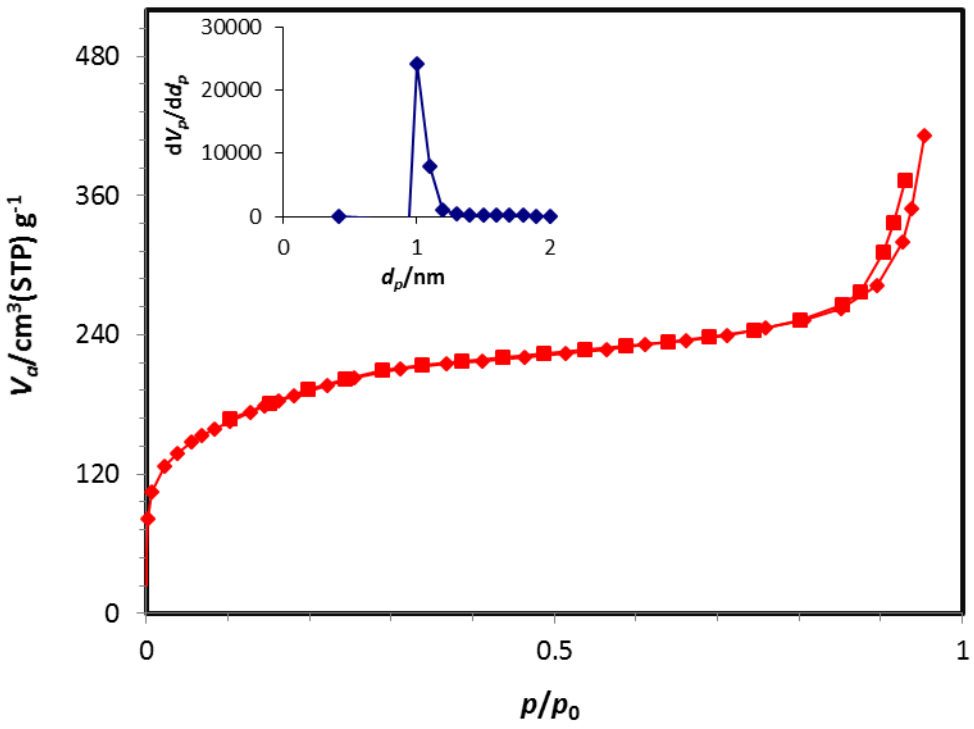

Figure 3.9 The nitrogen sorption isotherm of PSNsCOOH. Inset: MP-plot of PSNsCOOH.

The X-ray diffraction spectroscopy (XRD) was employed to characterize the ordered structure of PSNsCOOH. Figure 3.10 showed the Bragg diffraction peaks indexed as (100), (110), and (111) reflections. The spectrum showed the characteristic pattern for a two-dimensional (2D) hexagonal structure [35], which is the desired structure for drug delivery system due to their unique channel structure, high thermal stability, and good biocompatibility [81].

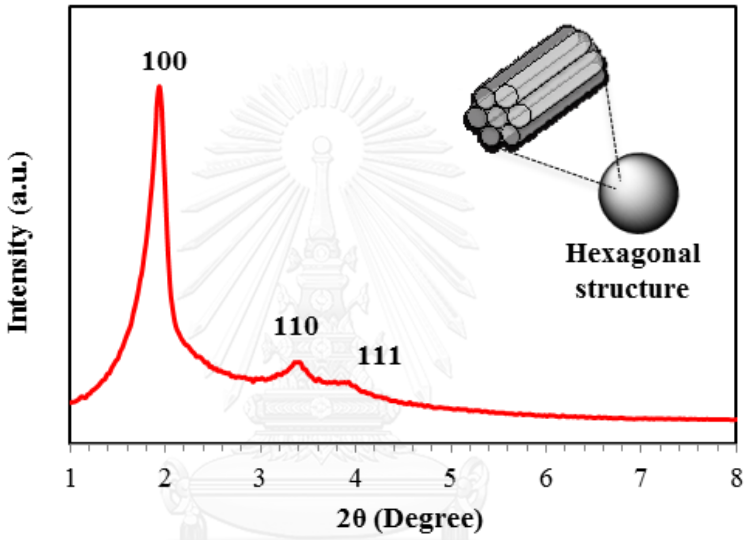

Figure 3.10 The XRD pattern of PSNsCOOH.

All characterization data suggested that PSNsCOOH would be a suitable drug vehicle

3.2.2 Cisplatin loading efficiency of PSNsCOOH

Cisplatin was incorporated into PSNsCOOH by a simple diffusion method. The amount of cisplatin incorporated was determined by ICP-AES, and loading efficiency was calculated from equation 1. Interestingly, the cisplatin loading efficiency of PSNsCOOH was dramatically increased to 59% (0.118 g of CDDP per 200 mg particles) compared to 7% of PSNs. The result can be concluded that the carboxyl group on PSNsCOOH showed high affinity with cisplatin, which was consistent with the published report [34]. Therefore, PSNsCOOH could improve the amount of loaded cisplatin and the particles would be further grafted with Cbl for targeted delivery system.

3.2.3 Synthesis and characterization of cobalamin-cisplatin adduct as a targeting molecule ([Cbl-CDDP]$^+$)

The [Cbl-CDDP]$^+$ was prepared following the published procedure (Scheme 3.4) [72]. The solution of $AgNO_3$ and cisplatin (1:1 mole ratio) was stirred in DI H_2O for 2 min. Then, the white precipitate was formed in the solution. This precipitation can be described as one chloro ligand removed from cisplatin and precipitated as AgCl(s). After that, H_2O rapidly substituted to form mono-aquacation species, which was more labile than normal cisplatin. The precipitate was then removed by centrifugation and Cbl was added into the supernatant. The color of solution changed from pale yellow to dark red. The cyano ligand of Cbl was proposed to substitute at aqua position of the cationic complex to form [Cbl-CDDP]$^+$.

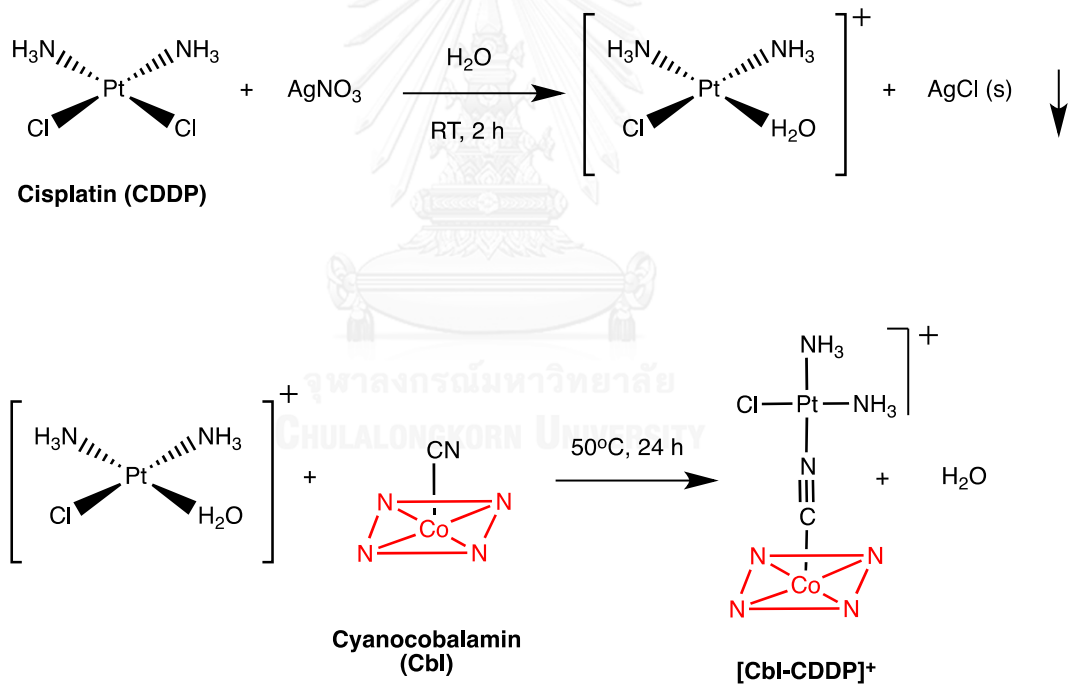

Scheme 3.4 Synthesis of [Cbl-CDDP]$^+$ as targeting molecule.

FT-IR spectroscopy was used to identify the coordination between cisplatin and the cyano group of Cbl. Figure 3.11 showed the spectra of free Cbl and Cbl-CDDP. The CN stretching peak of free Cbl appeared at 2134 cm^{-1} [82]. However, the band of CN stretching from [Cbl-CDDP]$^+$ shifted to 2190 cm^{-1}, with the previously reported

spectrum [72]. The result confirmed that the formation of $[Cbl\text{-}CDDP]^+$ adduct was successfully achieved.

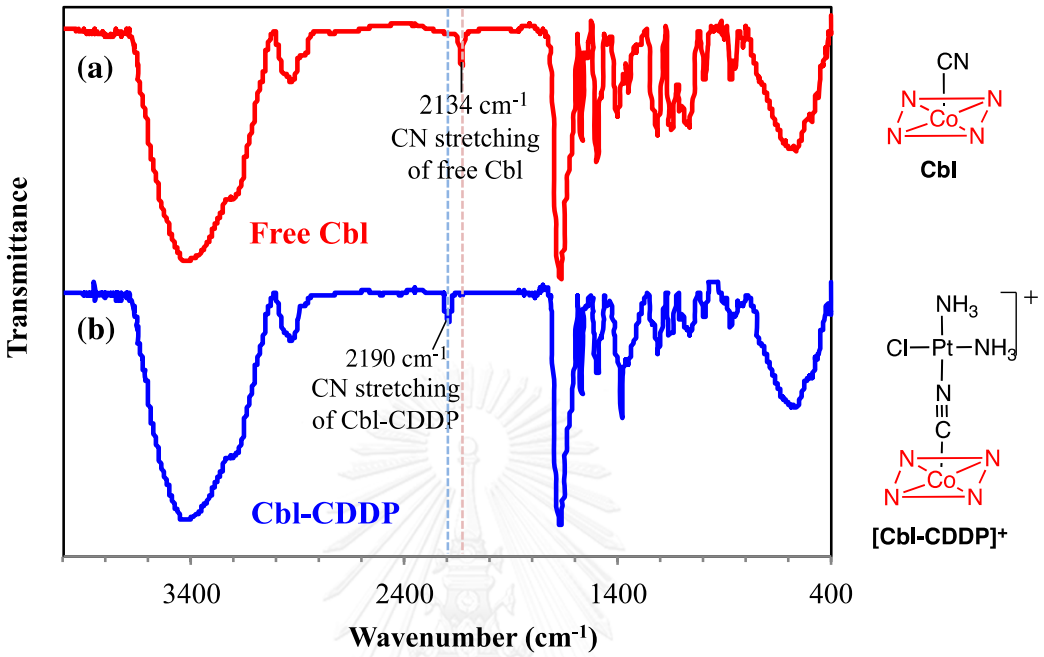

Figure 3.11 The FT-IR spectra of (a) Cbl and (b) $[Cbl\text{-}CDDP]^+$.

UV-visible spectroscopy was employed to identify the stability of Cbl in targeting ligand. The absorption spectra of free Cbl and $[Cbl\text{-}CDDP]^+$ in DI H_2O were shown in Figure 3.12. The characteristic absorption band of free Cbl appeared at 362 and 549 nm. The absorption bands of $[Cbl\text{-}CDDP]^+$ also appeared the same wavelength positions. This could be suggested that Cbl was stable and stayed intact in the adduct.

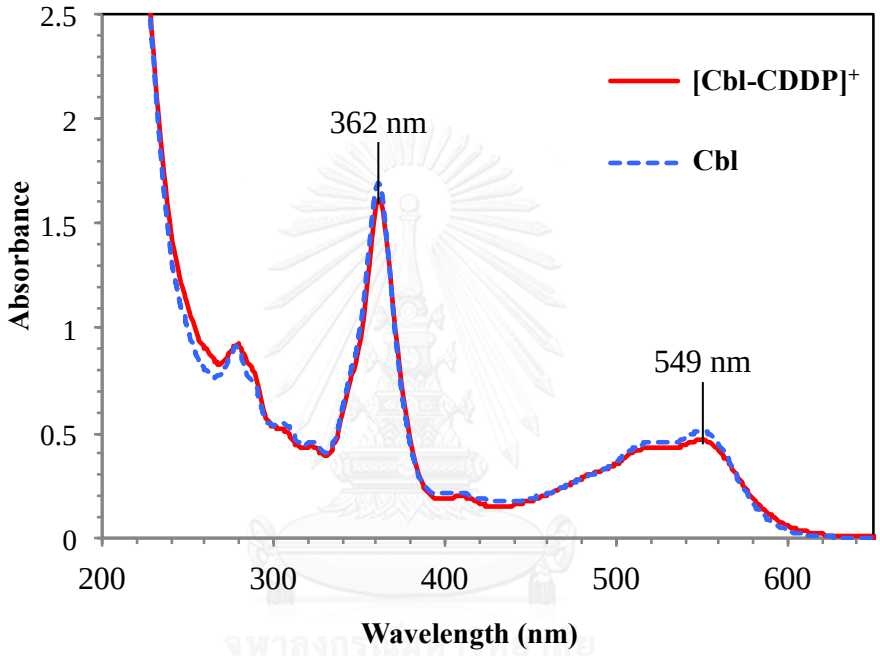

Figure 3.12 The UV-visible spectra of $[Cbl\text{-}CDDP]^+$ and free Cbl.

The molecular weight of $[Cbl\text{-}CDDP]^+$ was determined by ESI-MS. The solution was prepared in milli-Q water. The result compared between free Cbl and $[Cbl\text{-}CDDP]^+$. Free Cbl showed the peak of 1358. Meanwhile, $[Cbl\text{-}CDDP]^+$ appeared the peak of 1626, which was near to the exact mass [33]. The data was strongly confirmed that the product was $[Cbl\text{-}CDDP]^+$.

3.2.4 Synthesis and characterization of cobalamin-grafted cisplatin loaded carboxyl-porous silica nanoparticles (CDDP@CblPSNsCOOH)

To increase the selectivity of transportation, CDDP@PSNsCOOH were grafted with $[Cbl\text{-}CDDP]^{+}$ for targeted delivery (Scheme 3.5). The white solid particles of CDDP@PSNsCOOH were dispersed in the red Cbl-CDDP solution. In this step, we expected that the chloro ligand on the Pt center would be substituted by the carboxyl group of nanoparticles. After the reaction finished, the white particles turned into reddish product, which was indicative of Cbl grafting on the particles.

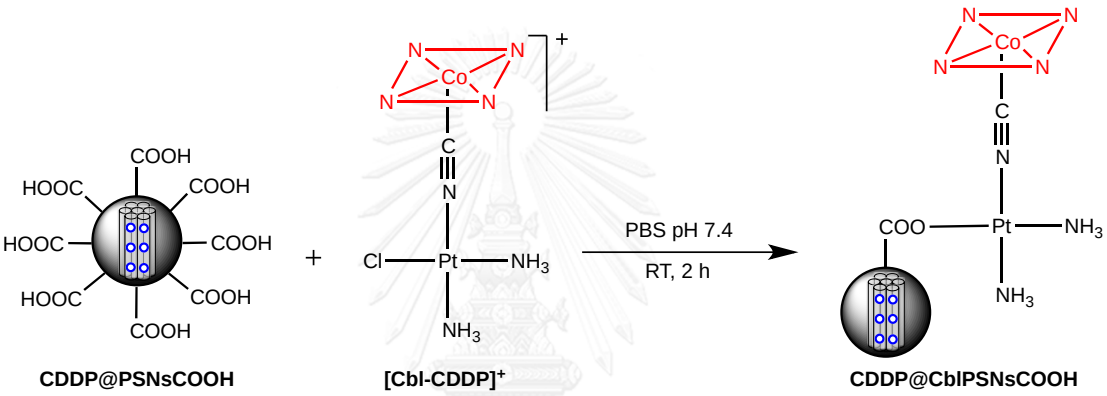

Scheme 3.5 Synthesis of CDDP@CblPSNsCOOH as novel drug delivery system.

The $[Cbl\text{-}CDDP]^+$ starting solution and supernatant were kept to determine the amount of $[Cbl\text{-}CDDP]^+$ grafted on the particles by UV-vis spectroscopy. The spectrum of $[83]^+]$ has a UV-vis feature at 361 and 549 nm [33]. The amount of $[Cbl\text{-}CDDP]^+$ was obtained from calibration curve (Figure 3.13). The grafting efficiency was calculated as the ratio between the net weight of $[Cbl\text{-}CDDP]^+$ grafted on the particles and weight of $[Cbl\text{-}CDDP]^+$ initially added, which was shown in Equation (2) [83]. The grafting efficiency of 20% was obtained.

Equation (2):

$$\text{Grafting efficiency}(\%) = \frac{\text{amount of } [\text{Cbl} - \text{CDDP}] \text{ grafted in particles (g)}}{\text{amount of } [\text{Cbl} - \text{CDDP}] \text{initially added (g)}} \times 100\%$$

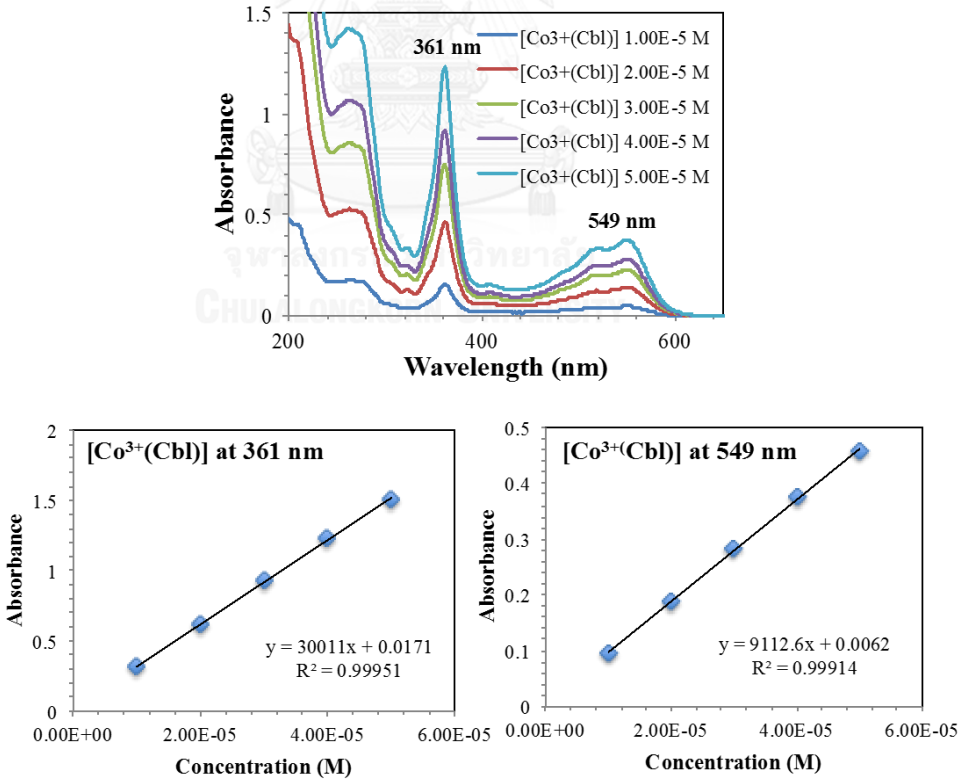

Figure 3.13 UV-vis spectra and calibration curve of $[(Co^{3+})[Cbl\text{-}CDDP]^+]$

Initially, we attempted to confirm the presence of Cbl on particle by DR-UV spectroscopy. However, the spectrum was too board such that the characteristic peaks of Cbl could not be identified. Hence, we turned to an alternative approach. In 2011, Sanchez et al. reported that $[Cbl\text{-}CDDP]^+$ or cis-$[PtCl(NH_3)_2Cbl]$ could be reduced by cobaltacene (Cp_2Co) to form cis-$[PtCl(NH_3)_2CN]$ and $[Co^{2+}(Cbl)]$ products (Scheme 3.6). It should be noted that UV-vis spectral features of $[Co^{2+}(Cbl)]$ are quite distinct from those of $[Cbl\text{-}CDDP]^+$ and $[Co^{3+}(Cbl)]$, so UV-vis spectroscopy can be used to monitor this reaction.

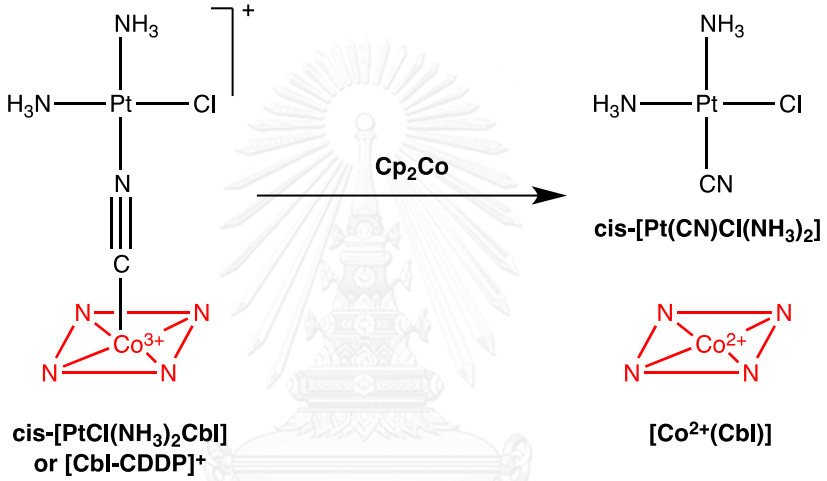

Scheme 3.6 Reduction of $[Cbl\text{-}CDDP]^+$ by cobaltocene (Adapted from Ref.[84].)

In our work, the reduction of $[Co^{3+}(Cbl)]$ was used to verify the coordination bond between Cbl and CDDP of CDDP@CblPSNsCOOH. However, cobaltocene is quite reactive and difficult to handle. Therefore, sodium borohydride ($NaBH_4$) was used as reducing agent in our experiment by following a published report [33]. Firstly, the reduction was tested with the free $[Co^{3+}(Cbl)]$ solution. After adding $NaBH_4$, the color of $[Co^{3+}(Cbl)]$ solution changed from red to orange-brown (Figure 3.14a) [85, 86]. UV-vis spectra changed upon reduction was also observed as shown in Figure 3.15a. These observations indicated the formation of $[Co^{2+}(Cbl)]$ [87]. Then, the reduction of CDDP@CblPSNsCOOH was carried. After adding $NaBH_4$, the color of solution turned orange-brown, which was similar to the free Cbl reaction (Figure 3.14b). The particles and supernatant were separated by centrifugation. UV-vis spectroscopy was also

performed to identify the cobalt species in the supernatant after reduction. As can be seen in Figure 3.15b, UV-vis spectrum of the supernatant was similar to the free [Co^{2+}(Cbl)] spectra, indicating that (Co^{3+})CblPSNsCOOH was reduced and gave [Co^{2+}(Cbl)] product. From the result, we proposed that the Cbl was cleaved from the particles at the β-ligand position upon reduction (Scheme 3.7) [35], leading to the observed [Co^{2+}(Cbl)] in the supernatant. In other words, the fact that [Co^{2+}(Cbl)] was observed after reduction of CblPSNsCOOH would imply the presence of Cbl on the particles in the first place.

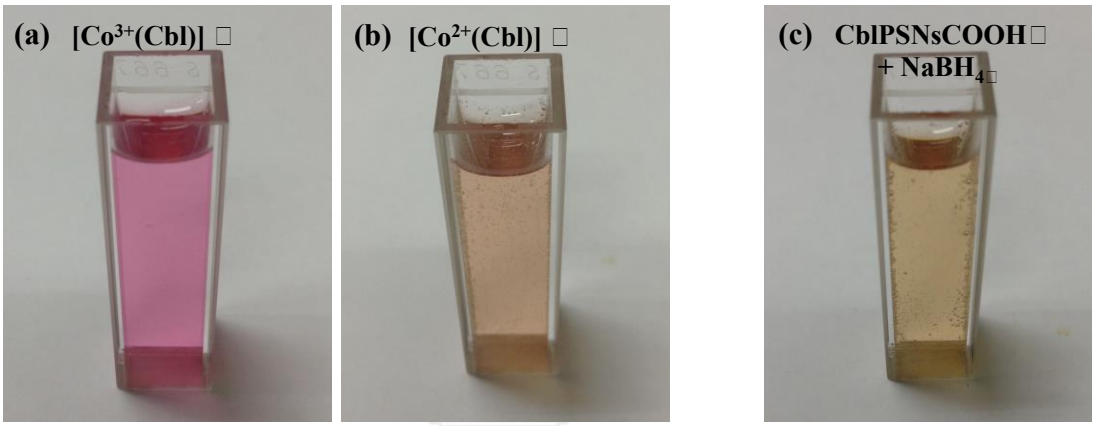

Figure 3.14 The solution of (a) [Co^{3+}(Cbl)], (b) [Co^{3+}(Cbl)] + $NaBH_4$, and (c) CblPSNsCOOH + $NaBH_4$

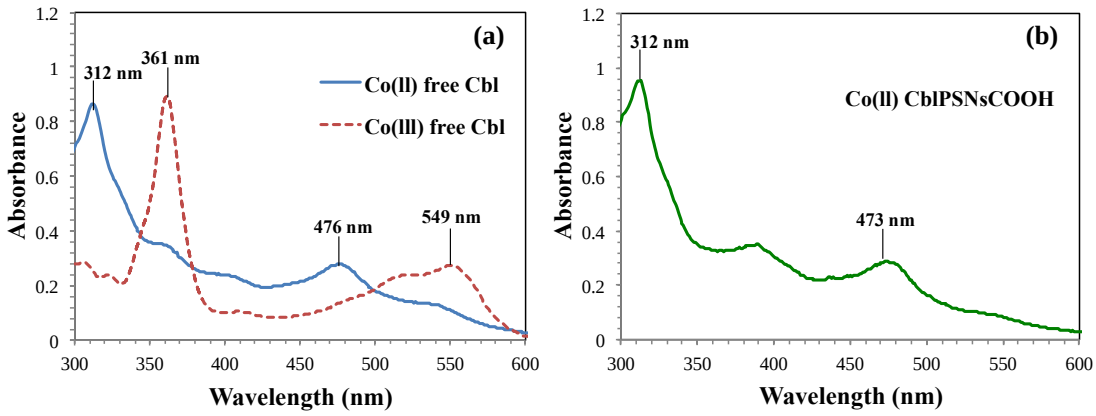

Figure 3.15 UV-visible spectra of (a) [Co^{3+}(Cbl)] and (b) [Co^{2+}(Cbl)] by $NaBH_4$

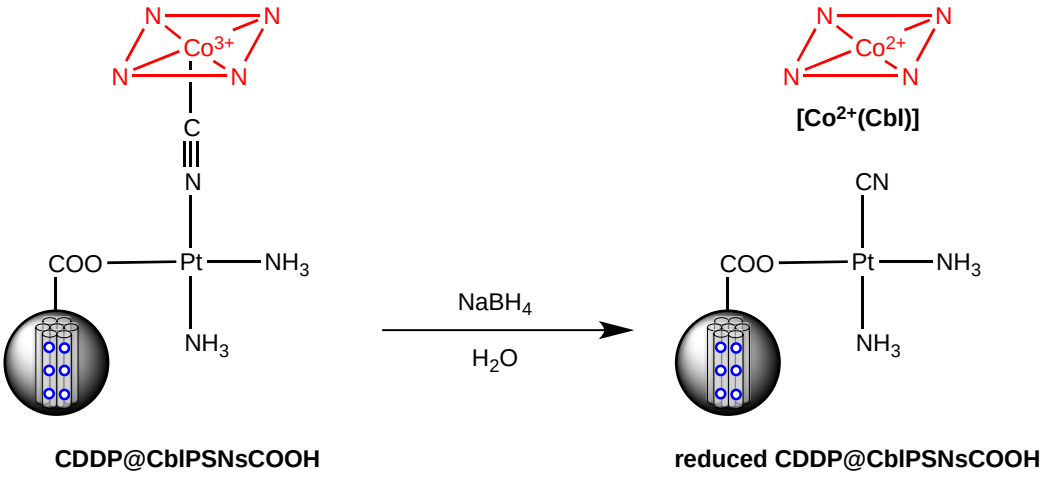

Scheme 3.7 The reduction of CDDP@CblPSNsCOOH by $NaBH_4$

From SEM images (Figure 3.16), the morphology of PSNsCOOH, CDDP@PSNsCOOH, and CDDP@CblPSNsCOOH was spherical in shape and monodispersed.

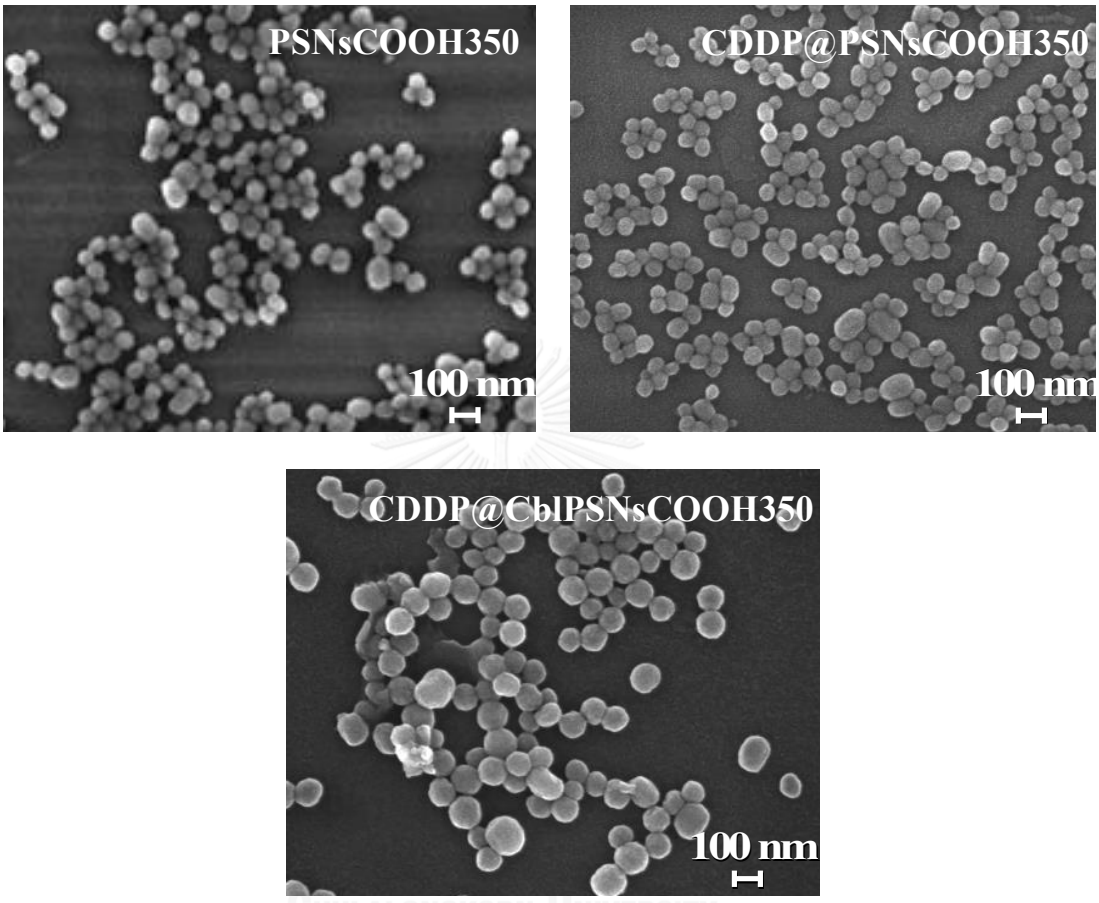

Figure 3.16 The SEM images of PSNsCOOH, CDDP@PSNsCOOH, and CDDP@CblPSNsCOOH

From Table 3.16, the DLS data showed the hydrated-diameter of three representative particles. The diameter of PSNsCOOH was 183 nm. Nevertheless, the particle size slightly increased to 230 nm after loading cisplatin. Moreover, the size of CDDP@CblPSNsCOOH expanded to 316 nm after grafting with $[Cbl\text{-}CDDP]^{+}$. CDDP@CblPSNsCOOH might still be applicable for drug delivery since particles in the similar size (300-600 nm) were demonstrated to be a successful drug delivery system and could be up taken by cancer cells [17].

Table 3. 2 The average size of the three representative nanoparticles and grafted-nanoparticles determined by DLS technique.

Particle name	Average diameter (nm)
PSNsCOOH	183 ± 8
CDDP@PSNsCOOH	230 ± 6
CDDP@CblPSNsCOOH	316 ± 6

3.3 Cisplatin releasing studies

3.3.1 The studies of cisplatin releasing from PSNsCOOH at pH 5.5 and pH 7.4

Generally, cancer cells are more acidic than normal tissue. The pH of tumor condition ranges from 5.5-7.6 [87]. In our research, the investigation of drug releasing profile of CDDP@PSNsCOOH was performed at pH 5.5 (cancer cell condition) and pH 7.4 (normal cell condition) using 0.1 M PBS buffer solution. Our assumption was that the cisplatin releasing from particles was pH-dependent. The quantification of cisplatin release was determined by ICP-AES. The cisplatin releasing efficiency was calculated from the ratio of cisplatin released into the supernatant and the initial amount of cisplatin loading in particles (0.118 g CDDP per 200 mg of particles), which was shown in equation (3) [88]. Figure 3.17 showed the concentration of cisplatin released from CDDP@PSNsCOOH matrix at pH 5.5 and 7.4 upon increasing the time.

Equation (3):

$$\text{Releasing efficiency}(\%) = \frac{\text{amount of CDDP released from particles (g)}}{\text{initial amount of CDDP in particles (g)}} \times 100\%$$

Table 3.3 Concentration of CDDP in the supernatant (50.00 mL) from CDDP@PSNsCOOH (200 mg) in PBS solution pH 5.5 and 7.4

Time (h)	Concentration of CDDP in supernatant (ppm)	
	pH 5.5	pH 7.4
1	208	168
2	336	286
3	394	344
4	436	400
5	466	414
6	528	460
8	563	520
12	618	574
24	672	614
48	712	638
72	714	668
96	736	692
120	776	712
168	774	728

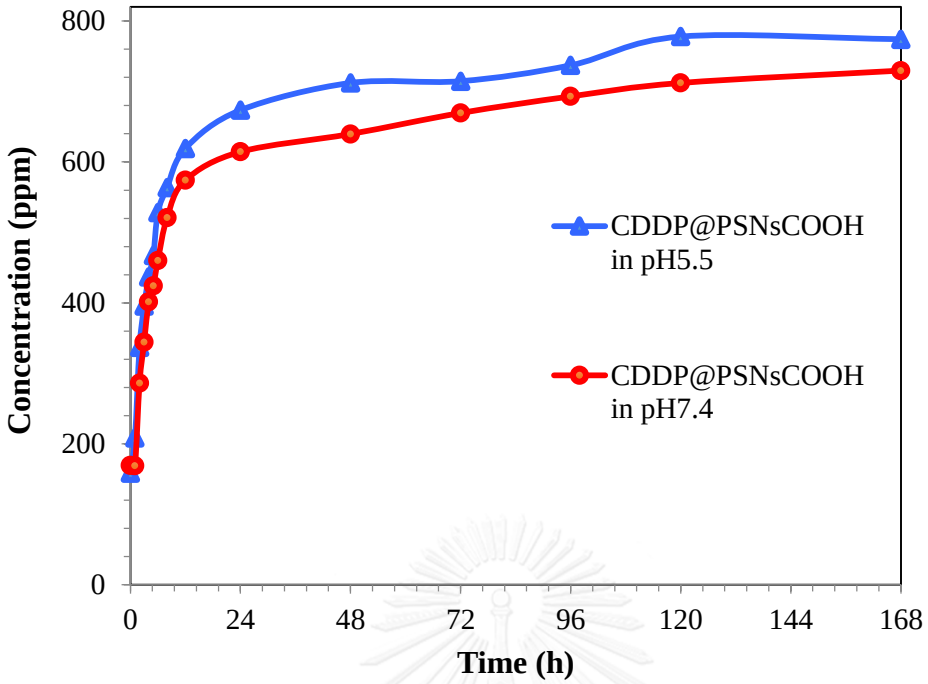

Figure 3.17 The cisplatin releasing behavior of CDDP@PSNsCOOH in 0.1 M PBS solution pH 5.5 and 7.4

The % cisplatin releasing from CDDP@PSNsCOOH matrix after 7 days at pH 5.5 and 7.4 were 33% and 31%, respectively. The cisplatin release was attributed to the protonation of the carboxy anion [34]. Consequently, the co-ordination between cisplatin and the carboxyl group was broken. Hence, cisplatin dissociated from the particle (Figure 3.18). The result indicated that PSNsCOOH could be used as cisplatin carrier and release into the cancer cells.

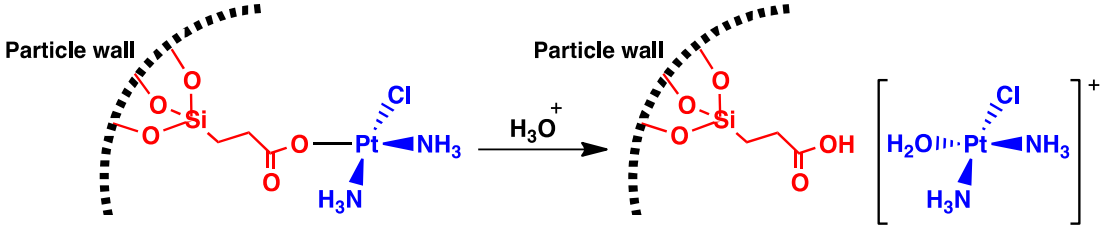

Figure 3.18 Proposed dissociation mechanism between cisplatin and PSNsCOOH (Adapted from Ref.[4].)

3.3.2 Mechanistic study of cisplatin releasing from CDDP@CblPSNsCOOH at pH 5.5

The cobalamin on the PSNsCOOH was expected to increase the specificity of delivery system. It was also expected to reduce the releasing rate of cisplatin during the transportation. We proposed that Cbl molecule could act as a gatekeeper, which was able to inhibit the release of cisplatin. The releasing behavior of CDDP@CblPSNsCOOH was compared to the CDDP@PSNsCOOH (Figure 3.19 a and b). The experiment was performed by ICP-AES. From Figure 3.19 a, CDDP@PSNsCOOH showed the sustained release in the matrix. The cisplatin releasing efficacy was 36%. However, only 10% of cisplatin was released from CblPSNsCOOH, suggesting that the drug was blocked by targeting ligand, Cbl. After that, we also studied the cisplatin releasing profile from particles after reducing Cbl by $NaBH_4$ (reduced CDDP@CblPSNsCOOH) (Figure 3.19c). We proposed that the reduction and cleavage of Cbl from the particles would induce the drug release. According to our assumption, the cisplatin releasing from reduced CDDP@CblPSNsCOOH was significantly raised up to 24%. The releasing behaviors of three representative particles indicated that grafting the targeting molecule on the drug carrier would help reduce the side effects of cisplatin in the circulation [89]. When the drug system is internalized into the cancer cells, $[Co^{3+}(Cbl)]$ will be reduced to $[Co^{2+}(Cbl)]$ by systematic enzymes and cleaved from the particles [90]. The naked-particles will be obtained. Thus, cisplatin could be released more easily in the cellular matrix.

Table 3.4 Concentration of CDDP in the supernatant (50.00 mL) from three representative particles (200 mg) in PBS solution pH 5.5

Time (h)	Concentration of CDDP in supernatant (ppm) from		
	PSNsCOOH	CblPSNsCOOH	reduced CblPSNsCOOH
1	202	62	90
2	294	80	134
3	366	136	176
4	400	114	252
5	462	84	326
6	206	142	356
7	534	112	206
8	550	116	328
12	602	114	414
16	634	128	440
20	668	210	482
24	692	130	486
36	726	174	486
48	746	226	534
72	780	208	580
96	802	204	520
120	834	202	588
144	846	218	538
168	846	236	552

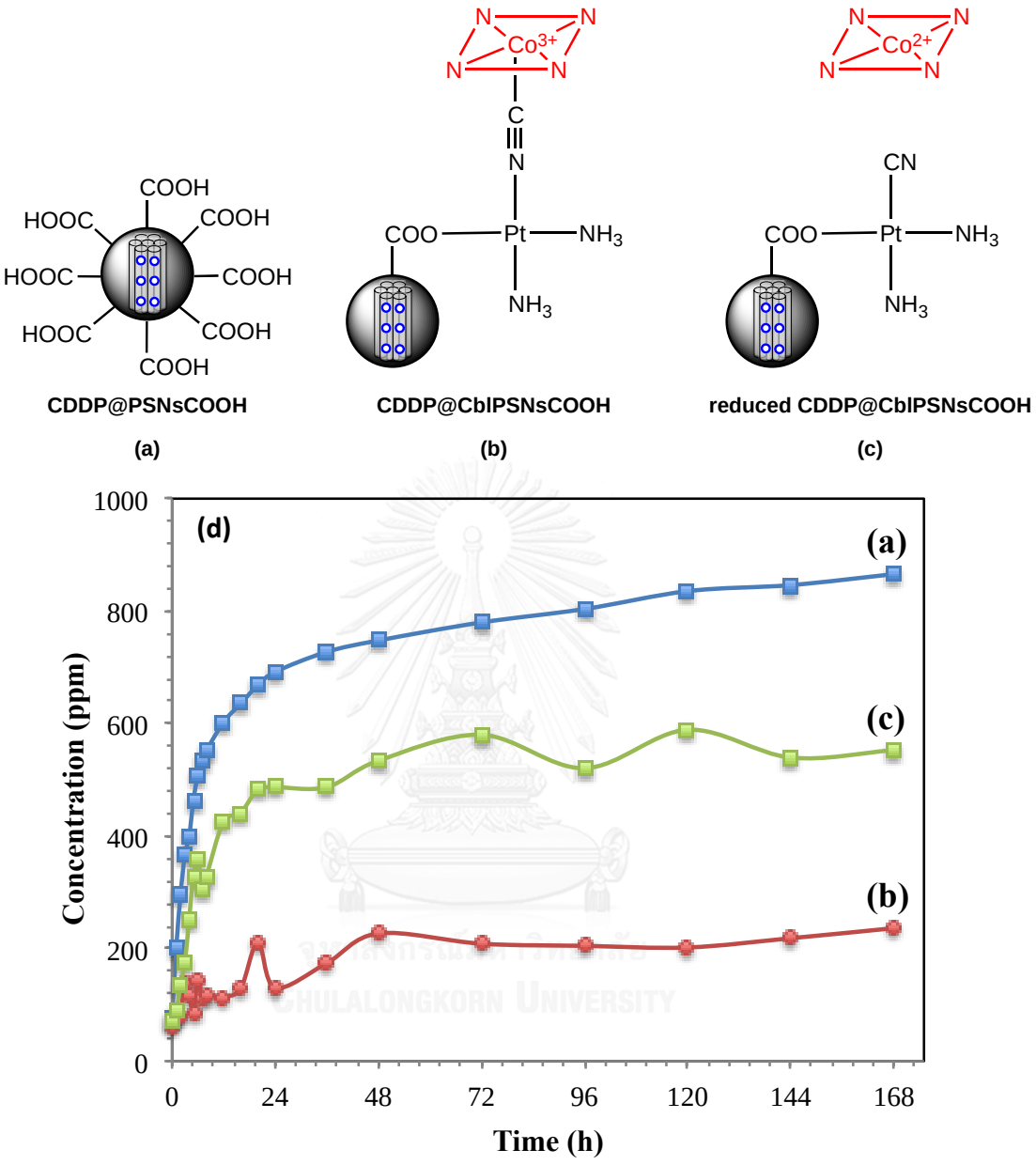

Figure 3.19 The model of cisplatin loaded in (a) PSNsCOOH, (b) CblPSNsCOOH, (c) CN-CDDP-PSNsCOOH, and (d) the cisplatin releasing behavior of three representative particles in 0.1 M PBS solution pH 5.5.

CHAPTER IV

CONCLUSION

In this work, we have developed a targeted anticancer drug delivery system based on cisplatin loaded cyanocobalamin-conjugated porous silica nanoparticles. The particles were spherical in shape and Cbl molecule could successfully grafted on the PSNs. However, the cisplatin loading efficiency of PSNs was only 7%, which could not conduct a releasing experiment. Hence, we have modified the functional group of particles from silanol to carboxyl group. The carboxyl-particles had been synthesized in 3 particles sizes namely PSNsCOOH250, PSNsCOOH300, and PSNsCOOH350. The hydrated-size of 3 representative particles was 347, 265, and 173 nm. We chose PSNsCOOH350 as drug carrier in this research due to the optimized size. The shape of PSNsCOOH were spherical and monodispersed. The pore size distribution was 1 nm. The pore volume and specific surface area were 0.637 cm^3g^{-1} and 694.82 m^2g^{-1}, respectively. The ordered structure of PSNsCOOH was hexagonal structure, which showed the good stability and biocompatibility. Moreover, the loading efficiency of cisplatin in carboxyl-particles was increased to 59%. Targeting molecule Cbl-CDDP was successfully conjugated on the carboxyl-particles by coordination bonding. Cisplatin released from PSNsCOOH had a sustained release pattern in both pH 5.5 and 7.4. In contrast, there was little cisplatin release from CblPSNsCOOH, suggesting the pore was blocked by Cbl. Nevertheless, it showed better release behavior after cutting off targeting molecule by reduction. Thus, we concluded that cisplatin loaded in cyanocobalamin conjugated carboxyl-porous silica nanoparticles had good potential to be targeted drug delivery for cancer therapy.

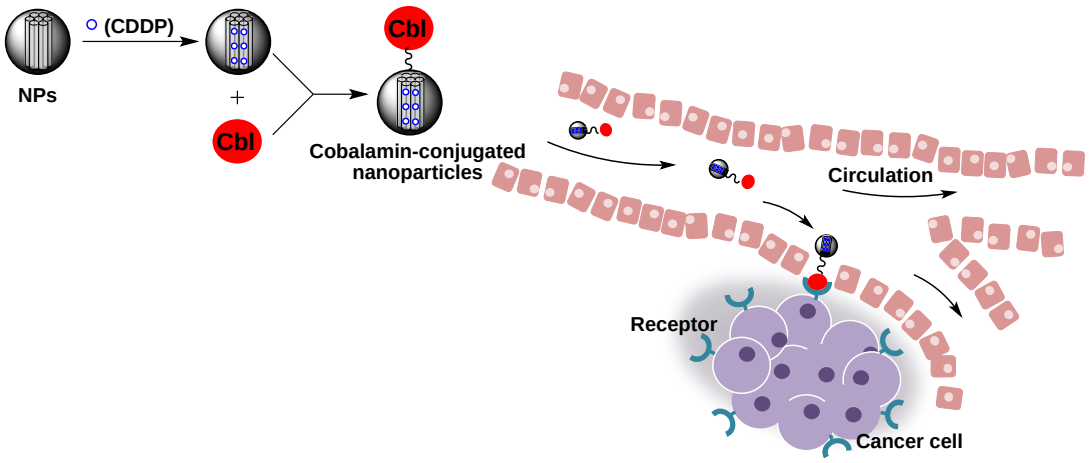

Figure 4.1 Proposed delivery mechanism of cisplatin loaded cobalamin-conjugated nanoparticles to cancer cells (Adapted from Ref.[91])

REFERENCES

[1] Liang, X.J., Chen, C., Zhao, Y., and Wang, P.C. Circumventing tumor resistance to chemotherapy by nanotechnology. Methods Mol. Biol. 596 (2010): 467-88.

[2] Pinhassi, R.I., et al. Arabinogalactan–Folic Acid–Drug Conjugate for Targeted Delivery and Target-Activated Release of Anticancer Drugs to Folate Receptor-Overexpressing Cells. Biomacromolecules 11 (2010): 294-303.

[3] Chandler, D. A materials for all seasons. MIT 53 (2009).

[4] Gu, J., Liu, J., Li, Y., Zhao, W., and Shi, J. One-Pot Synthesis of Mesoporous Silica Nanocarriers with Tunable Particle Sizes and Pendent Carboxylic Groups for Cisplatin Delivery. Langmuir 29 (2013): 403-410.

[5] Tao, Z., Xie, Y., Goodisman, J., and Asefa, T. Isomer-dependent adsorption and release of cis- and trans-platin anticancer drugs by mesoporous silica nanoparticles. Langmuir 26 (2010): 8914-24.

[6] Sysel, A.M., Valli, V.E., Nagle, R.B., and Bauer, J.A. Immunohistochemical quantification of the vitamin B12 transport protein (TCII), cell surface receptor (TCII-R) and Ki-67 in human tumor xenografts. Anticancer Res. 33 (2013): 4203-12.

[7] Argyo, C., Weiss, V., Bräuchle, C., and Bein, T. Multifunctional Mesoporous Silica Nanoparticles as a Universal Platform for Drug Delivery. Chem. Mater. 26 (2014): 435-451.

[8] Jacobsen, D.W. and Glushchenko, A.V. The transcobalamin receptor, redux. Blood 113 (2009): 3-4.

[9] Jain, K.K. Methods in Molecular Biology,. Drug. Deliv. (2008): 437.

[10] Lu, J., Liong, M., Li, Z., Zink, J.I., and Tamanoi, F. Biocompatibility, Biodistribution, and Drug-Delivery Efficiency of Mesoporous Silica Nanoparticles for Cancer Therapy in Animals. Small. 6 (2010): 1794-1805.

[11] Chidambaram, M., Manavalan, R., and Kathiresan, K. Nanotherapeutics to overcome conventional cancer chemotherapy limitations. J. Pharm. Sci. 14 (2011): 67-77.

[12] Dixit, N., Maurya, S.D., and Sagar, B.P. Sustained release drug delivery system. Ind. J. Res. Pharm. Biotech. 1 (2013): 305.

[13] Verraedt, E., Pendela, M., Adams, E., Hoogmartens, J., and Martens, J.A. Controlled release of chlorhexidine from amorphous microporous silica. J. Control. Release 142 (2010): 47-52.

[14] Rani, K. and Paliwal, S. A review on targeted durg delivery: its entire focus on advanced therapeutics and diagnostics. Sch. J. App. Med. Sci. 2 (2014): 328-331.

[15] Muller, R.H. and Keck, C.M. Challenges and solutions for the delivery of biotech drugs--a review of drug nanocrystal technology and lipid nanoparticles. J. Biotechnol. 113 (2004): 151-70.

[16] Agnihotri, J., Saraf, S., Khale, A. Targeting : New Potential Carriers for Targetted Drug Delivery System. Ind. J. Pharm. Educ. Res. 8 (2011).

[17] Zhu, Y., Fang, Y., and Kaskel, S. Folate-Conjugated Fe3O4@SiO2 Hollow Mesoporous Spheres for Targeted Anticancer Drug Delivery. J. Phys. Chem. C 114 (2010): 16382-16388.

[18] Tao, Z., Toms, B., Goodisman, J., and Asefa, T. Mesoporous silica microparticles enhance the cytotoxicity of anticancer platinum drugs. ACS Nano. 4 (2010): 789-94.

[19] Sikora, K. S. Advani, V. Koroltchouk, I. Magrath, L. Levy, H. Pinedo, G. Schwartsmann, M. Tattersall7 and S. Yan8et al. Essential drugs for cancer therapy: a World Health Organization consultation. Ann. Oncol. 10 (1999): 385-90.

[20] Jamieson, E.R. and Lippard, S.J. Structure, Recognition, and Processing of Cisplatin-DNA Adducts. Chem. Rev. 99 (1999): 2467-98.

[21] Alderden, R.A., Hall, M.D., and Hambley, T.W. The Discovery and Development of Cisplatin. J. Chem. Educ. 83 (2006): 728.

[22] Kelland, L. The resurgence of platinum-based cancer chemotherapy. Nat. Rev. Cancer 7 (2007): 573-84.

[23] Graham, L.A. Structure-Activity Relationships in Funtionalized Platinumacridine Anticancer Agents. Doctor of Philosophy, Chemistry Wake Forest University Graduate School of Arts and Sciences, 2012.

[24] Shi, Y., Liu, S.A., Kerwood, D.J., Goodisman, J., and Dabrowiak, J.C. Pt(IV) complexes as prodrugs for cisplatin. J. Inorg. Biochem. 107 (2012): 6-14.

[25] Jung, Y. and Lippard, S.J. Direct cellular responses to platinum-induced DNA damage. Chem. Rev. 107 (2007): 1387-407.

[26] Yang, D., van Boom, S.S., Reedijk, J., van Boom, J.H., and Wang, A.H. Structure and isomerization of an intrastrand cisplatin-cross-linked octamer DNA duplex by NMR analysis. Biochem. J. 34 (1995): 12912-20.

[27] Todd, R.C. and Lippard, S.J. Inhibition of transcription by platinum antitumor compounds. Metallomics 1 (2009): 280-291.

[28] Johnstone, T.C., Suntharalingam, K., and Lippard, S.J. The Next Generation of Platinum Drugs: Targeted Pt(II) Agents, Nanoparticle Delivery, and Pt(IV) Prodrugs. Chem. Rev. 116 (2016): 3436-3486.

[29] Florea, Ana-Maria, and Dietrich Büsselberg. "Cisplatin as an anti-tumor drug: cellular mechanisms of activity, drug resistance and induced side effects. Cancers (2011): 1351-1371.

[30] Siddik, Z.H. Cisplatin: mode of cytotoxic action and molecular basis of resistance. Oncogene 22 (2003): 7265-79.

[31] K.R, S.G., Mathew, B.B., Sudhamani, C.N., and Naik, H.S.B. Mechanism of DNA Binding and Cleavage. J. Biomed. and Biotechnol. 2 (2014): 1-9.

[32] Zhang, J.Z., et al. Facile preparation of mono-, di- and mixed-carboxylato platinum(IV) complexes for versatile anticancer prodrug design. Chemistry 19 (2013): 1672-6.

[33] Ruiz-Sanchez, P., Mundwiler, S., Spingler, B., Buan, N.R., Escalante-Semerena, J.C., and Alberto, R. Syntheses and characterization of vitamin B12-Pt(II) conjugates and their adenosylation in an enzymatic assay. J. Biol. Inorg. Chem. 13 (2008): 335-47.

[34] Gu, J., Su, S., Li, Y., He, Q., Zhong, J., and Shi, J. Surface Modification–Complexation Strategy for Cisplatin Loading in Mesoporous Nanoparticles. J. Phys. Chem. Lett. 1 (2010): 3446-3450.

[35] Rosenholm, J.M., Peuhu, E., Eriksson, J.E., Sahlgren, C., and Linden, M. Targeted intracellular delivery of hydrophobic agents using mesoporous hybrid silica nanoparticles as carrier systems. Nano. Lett. 9 (2009): 3308-11.

[36] Albanese, A., Tang, P.S., and Chan, W.C. The effect of nanoparticle size, shape, and surface chemistry on biological systems. Annu. Rev. Biomed. Eng. 14 (2012): 1-16.

[37] Slowing, I.I., Vivero-Escoto, J.L., Wu, C.-W., and Lin, V.S.Y. Mesoporous silica nanoparticles as controlled release drug delivery and gene transfection carriers. Adv. Drug. Deliv. 60 (2008): 1278-1288.

[38] Menz, W.J., Shraddha, S., George, B., Richard, K., Wolfgang, P., Markus, K. Synthesis of silicon nanoparticles with a narrow size distribution: A theoretical study. J. Aerosol. Sci. 44 (2012): 46-61.

[39] Kim, H.J., Matsuda, H., Zhou, H., and Honma, I. Ultrasound-Triggered Smart Drug Release from a Poly (dimethylsiloxane)–Mesoporous Silica Composite. Adv. Mater. 18 (2006): 3083-3088.

[40] Zhao, Y., Trewyn, B.G., Slowing, II, and Lin, V.S. Mesoporous silica nanoparticle-based double drug delivery system for glucose-responsive controlled release of insulin and cyclic AMP. J. Am. Chem. Soc. 131 (2009): 8398-400.

[41] Moulari, B., Pertuit, D., Pellequer, Y., and Lamprecht, A. The targeting of surface modified silica nanoparticles to inflamed tissue in experimental colitis. Biomaterials 29 (2008): 4554-60.

[42] Kwon, S., Singh, R.K., Perez, R.A., Abou Neel, E.A., Kim, H.-W., and Chrzanowski, W. Silica-based mesoporous nanoparticles for controlled drug delivery. J. Tissue Eng. 4 (2013).

[43] Trewyn, B.G., Whitman, C.M., and Lin, V.S.Y. Morphological Control of Room-Temperature Ionic Liquid Templated Mesoporous Silica Nanoparticles for Controlled Release of Antibacterial Agents. Nano. Lett. 4 (2004): 2139-2143.

[44] Che, S., Liu, Z., Ohsuna, T., Sakamoto, K., Terasaki, O., and Tatsumi, T. Synthesis and characterization of chiral mesoporous silica. Nature 429(6989) (2004): 281-284.

[45] Li, X., He, Q., and Shi, J. Global Gene Expression Analysis of Cellular Death Mechanisms Induced by Mesoporous Silica Nanoparticle-Based Drug Delivery System. ACS Nano. 8 (2014): 1309-1320.

[46] Burleigh, M.C., Dai, S., Hagaman, E.W., Barnes, C.E., and Xue, Z.L. Stepwise Assembly of Surface Imprint Sites on MCM-41 for Selective Metal Ion Separations. in Nuclear Site Remediation, American Chemical Society, 2000. pp. 146-158

[47] Eller, P.G. and Heineman, W.R. Nuclear Site Remediation. ACS Symposium Series. Vol. 778: American Chemical Society, 2000.

[48] Radu, D.R., Lai, C.-Y., Huang, J., Shu, X., and Lin, V.S.Y. Fine-tuning the degree of organic functionalization of mesoporous silica nanosphere materials via an interfacially designed co-condensation method. Chem. Commun. (10) (2005): 1264-1266.

[49] Lai, C.Y., Trewyn, B.G., Jeftinija, D.M., Jeftinija, K., Xu, S., Jeftinija, S., Lin. A mesoporous silica nanosphere-based carrier system with chemically removable CdS nanoparticle caps for stimuli-responsive controlled release of neurotransmitters and drug molecules. J. Am. Chem. Soc. 125 (2003): 4451-9.

[50] Slowing, I., Trewyn, B.G., and Lin, V.S. Effect of surface functionalization of MCM-41-type mesoporous silica nanoparticles on the endocytosis by human cancer cells. J. Am. Chem. Soc. 128 (2006): 14792-3.

[51] Slowing, II, Trewyn, B.G., and Lin, V.S. Mesoporous silica nanoparticles for intracellular delivery of membrane-impermeable proteins. J. Am. Chem. Soc. 129 (2007): 8845-9.

[52] Lu, J., Liong, M., Zink, J.I., and Tamanoi, F. Mesoporous silica nanoparticles as a delivery system for hydrophobic anticancer drugs. Small 3 (2007): 1341-6.

[53] Lu, C.W., Hung, Y., Hsiao, J.K., Yao, M., Chung, T.H., Lin, Y.S., Wu, S.H., Hsu, S.C., Liu, H.M., Mou, C.Y., Yang, C.S., Huang, D.M., Chen, Y.C. Bifunctional magnetic

silica nanoparticles for highly efficient human stem cell labeling. Nano. Lett. 7 (2007): 149-54.

[54] Chung, T.H.,Wu, S.H., Yao, M., Lu, C.W., Lin, Y.S., Hung, Y., Mou, C.Y., Chen, Y.C., Huang, D.M. The effect of surface charge on the uptake and biological function of mesoporous silica nanoparticles in 3T3-L1 cells and human mesenchymal stem cells. Biomaterials 28 (2007): 2959-66.

[55] Giri, S., Trewyn, B.G., Stellmaker, M.P., and Lin, V.S. Stimuli-responsive controlled-release delivery system based on mesoporous silica nanorods capped with magnetic nanoparticles. Angew. Chem. Int. Ed. Engl. 44 (2005): 5038-44.

[56] Vacha, R., Martinez-Veracoechea, F.J., and Frenkel, D. Receptor-mediated endocytosis of nanoparticles of various shapes. Nano. Lett. 11 (2011): 5391-5.

[57] Fedosov, S.N., Ruetz, M., Gruber, K., Fedosova, N.U., and Krautler, B. A blue corrinoid from partial degradation of vitamin B12 in aqueous bicarbonate: spectra, structure, and interaction with proteins of B12 transport. Biochemistry 50 (2011): 8090-101.

[58] Duncan, R., KopeckovÃ¡, P., Strohalm, J., Hume, I.C., Lloyd, J.B., and Kopecek, J. Anticancer agents coupled to N-(2-hydroxypropyl)methacrylamide copolymers. II. Evaluation of daunomycin conjugates in vivo against L1210 leukaemia. Br. J. Cancer 57 (1988): 147-156.

[59] Francis, M.F., Cristea, M., and Winnik, F.M. Exploiting the Vitamin B12 Pathway To Enhance Oral Drug Delivery via Polymeric Micelles. Biomacromolecules 6 (2005): 2462-2467.

[60] Wuerges, J., Geremia, S., Fedosov, S.N., and Randaccio, L. Vitamin B12 Transport Proteins: Crystallographic Analysis of β-axial Ligand Substitutions in Cobalamin Bound to Transcobalamin. IUBMB Life 59 (2007): 722-729.

[61] Allis, D.G., Fairchild, T.J., and Doyle, R.P. The binding of vitamin B12 to transcobalamin(II); structural considerations for bioconjugate design--a molecular dynamics study. Mol. Biosyst. 6 (2010): 1611-8.

[62] Bougrine, R., Masson, C., Hatier, R., Nexø, E., Nicolas, J.-P., and Gueant, J.-L. Receptor binding of transcobalamin II-cobalamin in human colon adenocarcinoma HT 29 cell line. J. Nutr. Biochem. 7 (1996): 397-402.

[63] Brada, N., Gordon, M.M., Wen, J., and Alpers, D.H. Transfer of cobalamin from intrinsic factor to transcobalamin II. J. Nutr. Biochem. 12 (2001): 200-206.

[64] Kapadia, C.R., Serfilippi, D., Voloshin, K., and Donaldson, R.M., Jr. Intrinsic factor-mediated absorption of cobalamin by guinea pig ileal cells. J. Clin. Invest. 71 (1983): 440-8.

[65] Youngdahl-Turner, P., Rosenberg, L.E., and Allen, R.H. Binding and Uptake of Transcobalamin II by Human Fibroblasts. J. Clin. Invest. 61 (1978): 133-141.

[66] Seetharam, B. Receptor-mediated endocytosis of cobalamin (vitamin B12). Annu. Rev. Nutr. 19 (1999): 173-95.

[67] Bauer, J.A., Morrison, B.H., Grane, R.W., Jacobs, B.S., Dabney, S., Gamero, A.M., Carnevale, K.A., Smith, D.J., Drazba, J., Seetharam, B., Lindner, D.J. Effects of interferon beta on transcobalamin II-receptor expression and antitumor activity of nitrosylcobalamin. J. Natl. Cancer. Inst. 94 (2002): 1010-9.

[68] Sysel, A.M., Valli, V.E., and Bauer, J.A. Immunohistochemical quantification of the cobalamin transport protein, cell surface receptor and Ki-67 in naturally occurring canine and feline malignant tumors and in adjacent normal tissues. Oncotarget. 6 (2015): 2331-2348.

[69] Tao, Z., Toms, B.B., Goodisman, J., and Asefa, T. Mesoporosity and functional group dependent endocytosis and cytotoxicity of silica nanomaterials. Chem. Res. Toxicol. 22 (2009): 1869-80.

[70] Zou, Z., He, D., Cai, L., He, X., Wang, K., Yang, X., Li, L., Li, S., Su, X. Alizarin Complexone Functionalized Mesoporous Silica Nanoparticles: A Smart System Integrating Glucose-Responsive Double-Drugs Release and Real-Time Monitoring Capabilities. ACS Appl. Mater. Interfaces. 8 (2016): 8358-66.

[71] Ma, Y., Xing, L., Zheng, H., and Che, S. Anionic–Cationic Switchable Amphoteric Monodisperse Mesoporous Silica Nanoparticles. Langmuir 27 (2011): 517-520.

[72] Mundwiler, S., Spingler, B., Kurz, P., Kunze, S., and Alberto, R. Cyanide-bridged vitamin B12-cisplatin conjugates. Chemistry 11 (2005): 4089-95.

[73] Kamaly, N., Xiao, Z., Valencia, P.M., Radovic-Moreno, A.F., and Farokhzad, O.C. Targeted polymeric therapeutic nanoparticles: design, development and clinical translation. Chem. Soc. Rev. 41 (2012): 2971-3010.

[74] Watanabe, M., Takamura, H., and Sugai, H. Preparation of Ultrafine Fe–Pt Alloy and Au Nanoparticle Colloids by KrF Excimer Laser Solution Photolysis. Nanoscale Res. Lett. 4 (2009): 565-573.

[75] Friedman, M. Applications of the Ninhydrin Reaction for Analysis of Amino Acids, Peptides, and Proteins to Agricultural and Biomedical Sciences. J. Agric. Food Chem. 52 (2004): 385-406.

[76] Punt, C.J.A., Nagtegaal, I.D., Van de Velde, C.J., Beets-Tan, R., Cats, A., Hoogerbrugge, N., Marijnen, C.A. Highlights from the seventh European Multidisciplinary Colorectal Cancer Congress (EMCCC) 2014. ecancermedicalscience 9 (2015): 497.

[77] Tang, H., Murphy, C.J., Zhang, B., Shen, Y., Van, K. E.A., Murdoch, W.J., Radosz, M. Curcumin polymers as anticancer conjugates. Biomaterials 31 (2010): 7139-49.

[78] Xu, C., Yuan, Z., Kohler, N., Kim, J., Chung, M.A., and Sun, S. FePt nanoparticles as an Fe reservoir for controlled Fe release and tumor inhibition. J. Am. Chem. Soc. 131 (2009): 15346-51.

[79] Stöber, W., Fink, A., and Bohn, E. Controlled growth of monodisperse silica spheres in the micron size range. J. Colloid Interface Sci. 26 (1968): 62-69.

[80] Valle-Vigón, P., Sevilla, M., and Fuertes, A.B. Carboxyl-functionalized mesoporous silica–carbon composites as highly efficient adsorbents in liquid phase. Microporous Mesoporous Mater. 176 (2013): 78-85.

[81] AlOthman, Z.A. and Apblett, A.W. Synthesis and characterization of a hexagonal mesoporous silica with enhanced thermal and hydrothermal stabilities. Appl. Surf. Sci. 256 (2010): 3573-3580.

[82] Santoro, G., Zlateva, T., Ruggi, A., Quaroni, L., and Zobi, F. Synthesis, characterization and cellular location of cytotoxic constitutional

organometallic isomers of rhenium delivered on a cyanocobalmin scaffold. Dalton Trans. 44 (2015): 6999-7008.

[83] Peng, M., Liao, Z., Zhu, Z., and Guo, H. A Simple Polymerizable Polysoap Greatly Enhances the Grafting Efficiency of the "Grafting-to" Functionalization of Multiwalled Carbon Nanotubes. Macromolecules 43 (2010): 9635-9644.

[84] Ruiz-Sanchez, P., Konig, C., Ferrari, S., and Alberto, R. Vitamin B(1)(2) as a carrier for targeted platinum delivery: in vitro cytotoxicity and mechanistic studies. J. Biol. Inorg. Chem. 16 (2011): 33-44.

[85] Hannibal, L., Smith, C.A., and Jacobsen, D.W. The X-ray Crystal Structure of Glutathionylcobalamin Revealed. Inorg. chem. 49 (2010): 9921-9927.

[86] Cheng, S. and Bobik, T.A. Characterization of the PduS Cobalamin Reductase of Salmonella enterica and Its Role in the Pdu Microcompartment. J. Bacteriol. 192 (2010): 5071-5080.

[87] Wike-Hooley, J.L., Haveman, J., and Reinhold, H.S. The relevance of tumour pH to the treatment of malignant disease. Radiother. Oncol. 2 (1984): 343-66.

[88] Nappini, S., Fogli, S., Castroflorio, B., Bonini, M., Baldelli Bombelli, F., and Baglioni, P. Magnetic field responsive drug release from magnetoliposomes in biological fluids. J. Mater. Chem. B 4 (2016): 716-725.

[89] Liu, Y., Wang, W., Yang, J., Zhou, C., and Sun, J. pH-sensitive polymeric micelles triggered drug release for extracellular and intracellular drug targeting delivery. Asian J. Pharmacol. 8 (2013): 159-167.

[90] Bonnitcha, P.D., Hall, M.D., Underwood, C.K., Foran, G.J., Zhang, M., Beale, P.J., Hambley, T.W. XANES investigation of the Co oxidation state in solution and in cancer cells treated with Co(III) complexes. J Inorg Biochem 100 (2006): 963-71.

[91] Sahub, C. Preparation of novel self-assembled coordination nanoparticles from surfactants and gadolinium ion to stabilize curcumin derivatives in buffered solution. Master degree Chemistry Chulalongkorn, 2013.

APPENDIX

VITA

Miss Nattanida Thepphankulngarm was born on 13rd March 1991 in Bangkok, Thailand. She has graduated with a high school diploma from Sarasas Witead Suksa School (Mathematics and Science Programme), Samutprakarn in2009. Then, she has graduated with the Bachelor's degree with a second class honor from faculty of Chemistry, department of Science, Chulalongkorn University in 2012. Afterwards, she was a Master degree student of Inorganic Chemistry and a member of Supramolecular Chemistry Research Unit (SCRU) at Chulalongkorn University under supervision of Professor Thawatchai Tuntulani and Dr. Pannee Leeladee.

Scholarship

2015 The 90th Anniversary of Chulalongkorn University Fund (Ratchadaphiseksomphot Endowment Fund), Chulalongkorn University

2014-2016 Research Assistant Scholarship, Chulalongkorn University

2013-2014 Teaching Assistant Scholarship, Chulalongkorn University

2012 Japan Student Services Organization Scholarship (JASSO)

Academic Experiences

2016 Poster presentation at The 10th Pure and Applied Chemistry International Conference 2016 (PACCON2016), 9-11 February 2016, Bitec, Bangkok, Thailand

2015 Poster presentation at Sokendai Asian Winter School Conference 2015 (AWS2015), 1-5 December, Nagoya, Japan

2012 Interchange for joint research and relationship in Japan Advanced Institute of Science and Technology School (JAIST) (Under supervision of Professor Noriyoshi Matsumi), 8 October-11 November,Ichikawa, Japan